ADIABATIC TRANSFER OF LIGHT IN A DOUBLE CAVITY

ADIABATIC TRANSFER OF LIGHT IN A DOUBLE CAVITY

By

NICK MILADINOVIC, B.Sc.

A Thesis
Submitted to the School of Graduate Studies
in Partial Fulfillment of the Requirements
for the Degree
Master of Science

McMaster University
©Copyright by Nick Miladinovic, 2011.

MASTER OF SCIENCE (2011)
(Physics)

McMaster University
Hamilton, Ontario

TITLE: Adiabatic Transfer of Light in a Double Cavity

AUTHOR: Nick Miladinovic, B.Sc.(University of Toronto)

SUPERVISOR: Dr. D. O'Dell

NUMBER OF PAGES: vi, 54

Abstract

The goal of this thesis is to perform a simple theoretical analysis of the problem of two optical cavities coupled by a common mirror which is movable. The mirror position controls the electromagnetic mode structure of the double cavity. Modes can be transferred from one side to the other by moving the mirror, thereby allowing deterministic and on-demand transfer of photons between two cavities. By mapping the Maxwell wave equation onto the Schrödinger wave equation, we are able to make use of the Landau-Zener result for the transition probability at an avoided crossing to obtain the conditions for adiabatic transfer.

Acknowledgements

I would first and foremost like to thank my supervisor, Duncan O'Dell, for his support and guidance over the last two years. Thanks to my office mates, and in particular to Faiyaz Hasan for living the wild life. Thanks to Prasana, Alan, Louca, and Phil for their guidance and friendship. A big thank you to Rory Woods for being an amazing friend during the past couple years - keep working on your starcraft. I want to also say how grateful I am to the staff at Mcmaster. Dr.Shi, Dr.Lee, Dr. Sorensen and Dr.Chen have in particular helped me out significantly during my time here. I acknowledge the time and effort of my committee team comprising of Dr.O'Dell, Dr.Shi, and Dr.Haugen and thank them for their patience and support. Most importantly, I want to thank my friends and family back in Toronto. Dave and Viet have been, and always will be my true motivation to excel in all walks of life. I am lucky to have an amazingly supportive family and group of friends. Finally, I wouldn't be here without the wisdom and input I have received from Arjun, Chris Lam, and Betty. Thank you all!

Contents

1 Introduction **1**

1.1 Motivation and Approach 1

1.2 δ-function mirror model 3

2 Static Solutions of Maxwell's Wave Equation **5**

2.1 Solutions of Maxwell's Wave Equation 5

2.2 Analysis of the Mode Structure 7

2.2.1 Mode properties 7

2.2.2 Similarities and Differences between the Schrödinger and Maxwell Wave Equations 9

2.2.3 Mode Approximation 10

2.3 Transfer Ratio 11

3 Quantum Considerations **17**

3.1 Landau-Zener Transitions 17

3.2 From Maxwell to Schrödinger 19

3.3 Quantization 22

4 Beyond the δ-function model **25**

4.1 Finite Width Mirror 25

4.2 Experimental realizability 29

5 Future Work **35**

6 Conclusion **37**

Appendices **37**

A Derivation of maximal amplitude wavenumber approximation **39**

B Transmission and Reflection for lossless dielectric mirrors **43**

C The diabatic basis **47**

D Analytic Approximation for Wavenumbers **49**

E The Maxwell wave equation in a moving dielectric **51**

Chapter 1

Introduction

1.1 Motivation and Approach

Optomechanical systems which couple electromagnetic radiation fields with mechanical degrees of freedom offers a novel regime of research in quantum information and communication technologies (QICT). One of the outstanding challenges facing quantum information proposals based on cavity quantum electrodynamics (CQED) is the problem of transferring photons between cavities in an efficient and robust manner [1]. One of the most promising ideas in QICT involves a network of neutral atoms isolated inside a series of optical cavities, and connected via optical fibers [2]. The atoms in each cavity act as a node in a quantum network made up of many such cavities. Quantum networks provide a way to solve the problem of scalability in quantum information processing, scalability being one of the Divincenzo criteria for the realization of a quantum computer [3].

A simple system which encapsulates some of these ideas is the double cavity - illustrated in Figure 1.1. In this thesis I consider the adiabatic transfer of light between two cavities by translating the cavity mirrors. By changing the length of the cavities we change the structure of the electromagnetic modes, thereby allowing a mode which is initially localized in one cavity to be smoothly transferred into the other cavity. This simple double cavity model allows for a straightforward analysis of the conditions for adiabatic transfer, as well as allowing for a number of analytic results to be obtained. The focus of the thesis will be on the study of the global normal modes of Maxwell's equations, and will be free of atoms. Future work will introduce atoms into the cavities, which will interact with the photons. If the mirrors are positioned in such a way as to create a resonant global mode which is strongly localized in one of the cavities, then a photon emitted by one of the atoms will be found in that resonant mode. On can then shift mirror positions, and adiabatically transfer the photon to the adjacent cavity where it will interact with the atoms there. The strength in setting up the mode structure in such a way comes from the efficiency of the transfer. Suppose that instead the mirrors were positioned arbitrarily. The emitted photon would then be in a superposition of

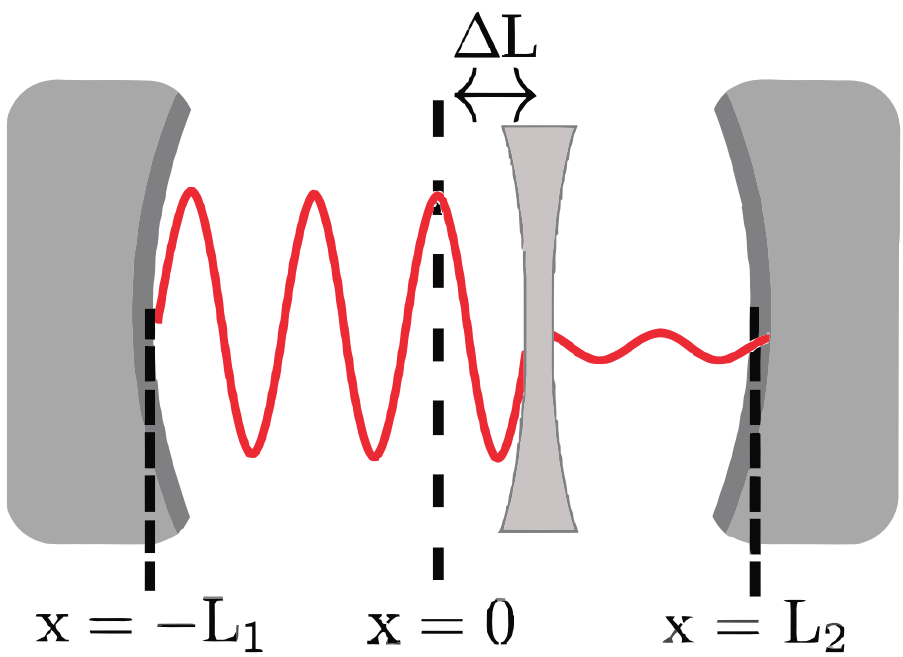

Figure 1.1: Double cavity setup consisting of two perfectly reflecting mirrors, along with a partially transmissive common central mirror.

global modes which would lead to a sloshing back and forth of the photon between the cavities. This would then necessitate the need for extremely precise timings in the experiment to achieve an efficient transfer. This insensitivity to timing makes the proposed method an appealing candidate for achieving efficient, and robust transfer of photons between cavities.

The thesis will be divided into several chapters. In the first section we introduce a δ-potential model for the double cavity system. This simplifies the mathematics and allows for the derivation of a number of analytic results. In the second section we examine the normal global mode structure whose frequencies form a network of avoided crossing pairs. As the cavity size is extremely small, the spacings between energy levels is sufficiently large that we may focus on a single pair of normal modes. This allows us to treat the problem as a two state system. In the third section, we treat the time-dependent cavity electrodynamics from first principles, by starting with Maxwell's wave equation, from which a Hamiltonian is derived. It is shown that to lowest order in mirror speed, the Maxwell wave equation gives a first order in time equation of motion for the classical Maxwell field that has a mathematical resemblance to the time-dependent Schrödinger equation [7]. This then allows the mapping of the Maxwell wave equation onto the Schrödinger equation. We are therefore able to apply the Landau-Zener result [10, 11, 12], familiar from non-relativistic quantum mechanics,

to the calculation of the coupling between classical Maxwell modes induced by the motion of the mirrors. In the fourth section, we consider a more realistic model in which the central mirror is given a finite width, and give the conditions for which the δ-model matches the finite model. We also consider the experimental realizability of the scheme. The last section will discuss future work, such as extending the system to a triple cavity system, and the introduction of atoms.

1.2 δ-function mirror model

Consider a double cavity formed from two end mirrors along with a common mirror located between them, as shown Figure 1.1. The end mirrors are assumed to be much more reflective than the central mirror so that the loss of light from the double cavity is negligible during the time taken for the light to be transferred from one side to the other. The stringent conditions this places on an experiment will be examined in Section 4.2. The common mirror is given a small, but finite transmission which couples the local modes of the left and right cavities. The end mirrors are kept static, while we allow the common mirror to shift.

A simple theoretical model describing a double cavity has been given in a classic paper by Lang, Scully and Lamb [13]. For the purposes of solving Maxwell's wave equation in the double cavity, they treated the end mirrors as perfect reflectors and the central mirror as a thin slab of dielectric material with a permittivity η and thickness δ. We take the limits in which

$$\eta \to \infty \qquad \delta \to 0 \qquad \eta\delta \to \alpha \tag{1.1}$$

Here α is a finite parameter with a dimension of length. It encapsulates the transmissitivity of the central mirror, where higher values of α correspond to higher reflectivity, see the Appendices for more details. We may model this potential using a Dirac δ-function spatial profile. The dielectric permittivity function is of the form

$$\varepsilon(x) = \begin{cases} \varepsilon_0(1+\alpha\delta(x)) & -L_1 < x < L_2 \\ \infty & \text{elsewhere} \end{cases} \tag{1.2}$$

where $x = -L_1$, and $x = L_2$ are the positions of the end mirrors. The total length of the double cavity is denoted by $L \equiv L_1 + L_2$, and we also define $\Delta L \equiv L_1 - L_2$ to be the displacement of the common mirror from the center. Maxwell's wave equation for the electric field in the double cavity is given by (see Appendix E for remarks on this)

$$\frac{\partial^2 \mathcal{E}(x,t)}{\partial x^2} - \mu_0\varepsilon_0(1+\alpha\delta(x))\frac{\partial^2 \mathcal{E}(x,t)}{\partial t^2} = 0 \ . \tag{1.3}$$

Chapter 2

Static Solutions of Maxwell's Wave Equation

2.1 Solutions of Maxwell's Wave Equation

We write the solutions to the Maxwell wave equation as $\mathcal{E}_m(x,t) = U_m(x)\exp(-i\omega_m t)$, where $\omega_m = k_m/\sqrt{\varepsilon_0\mu_0}$ is the angular frequency and $m = 1, 2, 3\ldots$ is an integer labeling the modes. The modes can be chosen to be orthonormal in the Sturm-Liouville sense by ensuring that they obey

$$\frac{1}{\varepsilon_0}\int_{-L_1}^{L_2} \varepsilon(x)U_m(x)U_n(x)dx = \delta_{mn} \ . \tag{2.1}$$

Inserting the above form for $\mathcal{E}(x,t)$ into Eq. (1.3) gives

$$\frac{\mathrm{d}^2U_m(x)}{\mathrm{d}x^2} + k_m^2(1+\alpha\delta(x))U_m(x) = 0 \ . \tag{2.2}$$

Solutions satisfying the boundary conditions $U_m(-L_1) = U_m(L_2) = 0$ are given by

$$U_m(x) = \begin{cases} A_m \sin(k_m(x+L_1)) & -L_1 \leq x \leq 0 \\ B_m \sin(k_m(x-L_2)) & 0 < x \leq L_2 \ . \end{cases} \tag{2.3}$$

The amplitudes A_m and B_m are determined by enforcing appropriate boundary conditions at the central mirror.

Assuming the electric field is continuous across the δ-mirror, so that

$$U_m(0^+) = U_m(0^-) \tag{2.4}$$

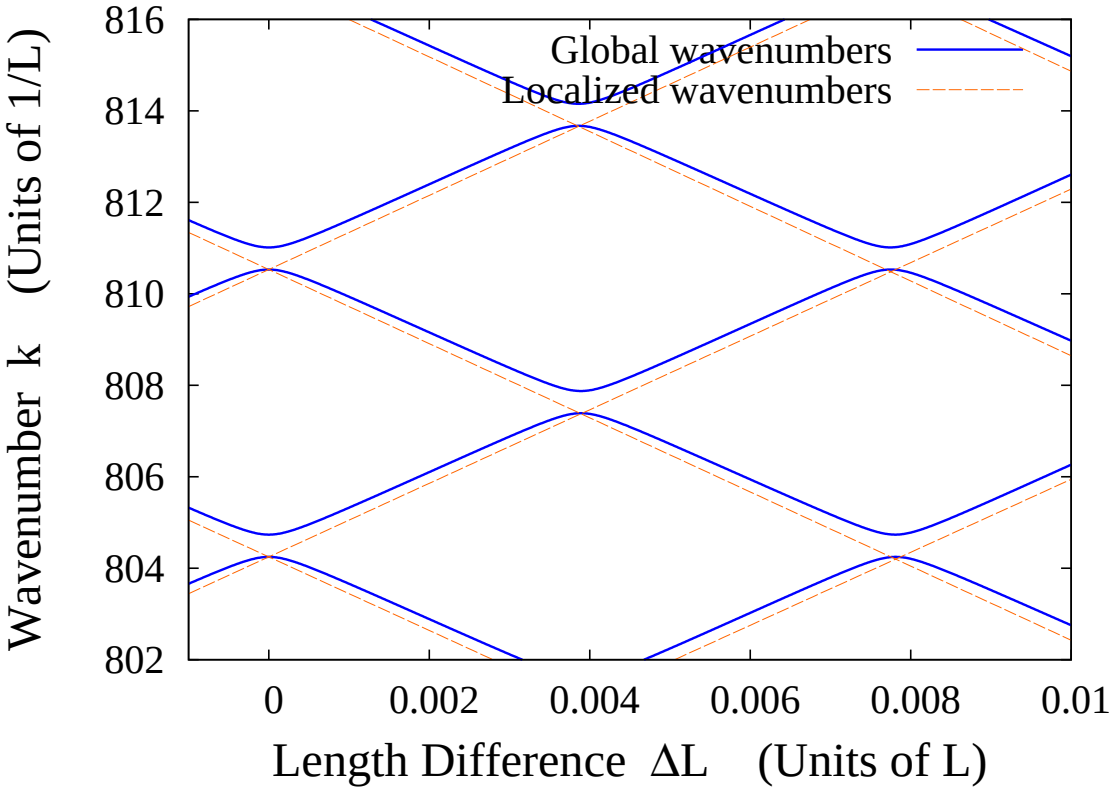

Figure 2.1: This figure shows the allowed modes in a double cavity, as specified by their vacuum wave numbers k_m, and plotted as a function of the displacement ΔL of the common mirror from the center of the cavity. The wavenumbers are obtained by solving the transcendental equation (2.7). When the reflectivity of the common mirror is infinite ($\alpha \to \infty$), we obtain the localized modes (thin dashed lines), which are trapped on one side or the other of the mirror. When the reflectivity is finite we obtain the global modes (solid curves) which feature avoided crossings. The total cavity length is set at $L = 1 \times 10^{-4}$m, and the global curves have $\alpha = 1 \times 10^{-6}$m, which translates to a transmission probability of the common mirror of about 4%. Note that we are in the wavelength range of $\lambda = 780$ (nm). This range corresponds to the wavelengths used in Rubidium lasers.

We can integrate Eq. (2.2) over a vanishingly small interval containing the mirror to find

$$U'_m(0^+) - U'_m(0^-) = -\alpha k_m^2 U_m(0) \tag{2.5}$$

We therefore see that although the electric field is continuous, its spatial gradient has a finite discontinuity at the boundary. The effects of this discontinuity will be seen in Section 4.1.

Combining the boundary conditions one is led to the following transcendental equation for the wavenumbers k_n of the allowed modes [13]

$$\tan(k_m L_2) = \frac{\tan(k_m L_1)}{\alpha k_m \tan(k_m L_1) - 1} \ . \tag{2.6}$$

This equation can in general only be solved numerically, although we shall find analytic solutions valid in certain regimes. For this purpose, we rearrange it into the form

$$\cos(k\Delta L) - \cos(kL) = 2\,\frac{\sin kL}{\alpha k}\ . \tag{2.7}$$

The advantage of this form is that in the optical regime where k becomes large, the sinc function on the right hand side becomes small. Providing α is not too small, the left hand side can then be expanded around its roots and this permits approximate analytic solutions (Eqns (2.14) and (2.13) below).

2.2 Analysis of the Mode Structure

2.2.1 Mode properties

Let us consider first the situation in which the common mirror is perfectly reflecting ($\alpha \to \infty$). In this scenario the left and right sides of the double cavity are uncoupled. The modes would then be specified by the wavenumbers $k_n = 2n\pi/(L \pm \Delta L)$, which come in pairs that cross at $\Delta L = 0$, and are plotted as the thin lines in Figures 2.1 and 2.2. The solution which decreases as ΔL is increased corresponds to the mode trapped on the left hand side of the mirror, and the solution which increases corresponds to the mode trapped on the right hand side of the mirror. We shall henceforth refer to the wavenumbers in the perfectly reflecting case as *localized* solutions. It is important to emphasize that the integer n used here identifies the paired solution, and not individual eigenmodes. For each n, there is a corresponding even and odd mode. For the remainder of the thesis, we will be using the n paired solution convention to identify wavenumbers.

To find the modes when the coupling between the two sides of the cavity is finite, one must solve Eq. (2.7) for k, with α appropriately chosen to give the desired reflectivity of the common mirror. As shown in Appendix B, the reflection probability from the δ-mirror is given by

$$R = \frac{k^2\alpha^2/4}{1 + k^2\alpha^2/4}\ . \tag{2.8}$$

We shall refer to solutions of Eq. (2.7) for finite α as *global* solutions, because they extend throughout the double cavity, and they are plotted as the thick curves in Figures 2.1 and 2.2. As can be seen in these figures, the effect of the coupling is to turn the crossings into avoided crossings.

At $\Delta L = 0$ the cavity is symmetric about the central mirror and so the solutions of Maxwell's wave equation must have well defined parity: for each n we find a pair of modes, one of which is even and the other odd. As the common mirror is moved away from the center of the cavity the global modes lose their well defined parity, but we shall continue to label them as "even" and "odd" because they retain much of their character providing we are in the neighborhood of an avoided

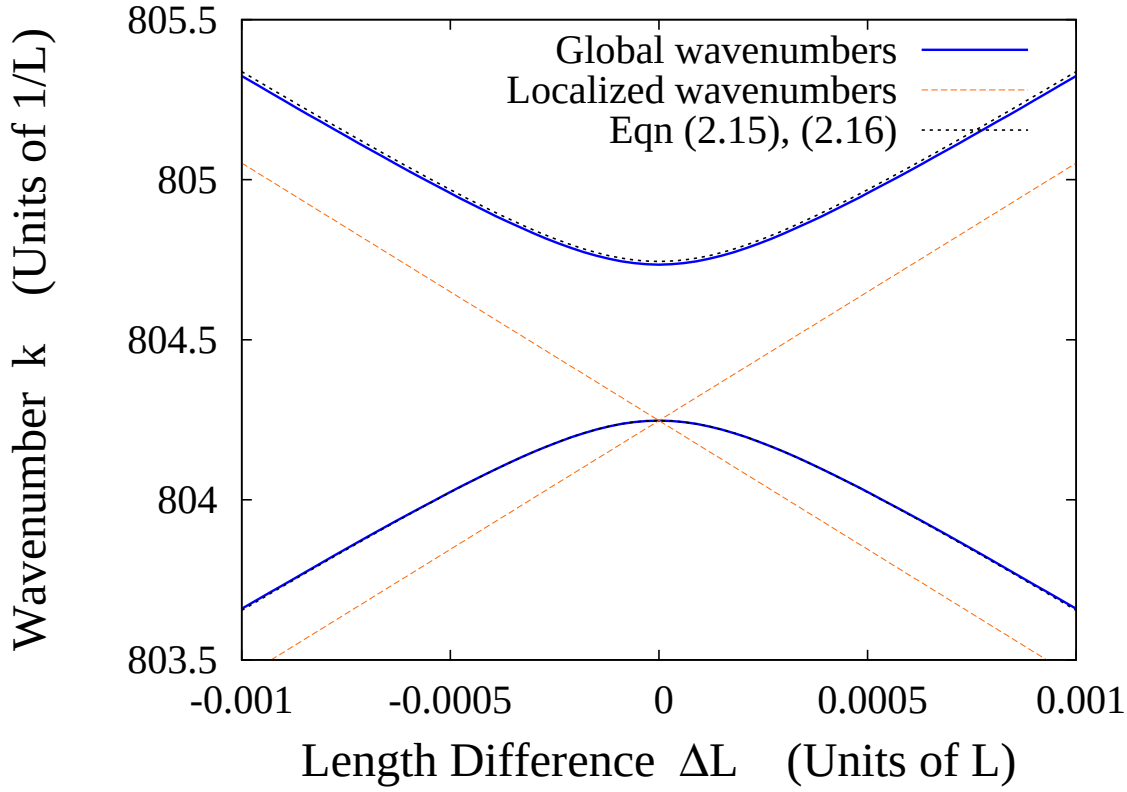

Figure 2.2: A zoom-in of an avoided crossing from Figure 2.1 corresponding to $n = 128$. The exact numeric solutions to Eq. (2.7) are plotted as solid (blue) curves, the localized solutions are plotted as dashed (red) curves, and the approximate analytic solutions given by Eqns. (2.15) and (2.16) are plotted as short dashed (black) curves. In contrast to the double well problem in quantum mechanics, the lower solid curve corresponds to the odd global solution. The localized solution lines cross the odd global solution curve at the avoided crossing.

crossing (see Figure 2.3). It is interesting to note that unlike the mode structure obtained from the Schrödinger equation for the double well problem, for all n the odd mode lies lower than the even mode. It is tempting here to use the term "lower energy", however classically the energy density is given by

$$\text{Energy density} = \frac{\epsilon_0}{2}\mathcal{E}^2(x,t) \tag{2.9}$$

This begs the question - what are the similarities and differences between the Schrödinger equation and the Maxwell wave equation?

2.2.2 Similarities and Differences between the Schrödinger and Maxwell Wave Equations

We begin by considering the Maxwell wave equation in a one dimensional medium with refractive index $n_r(x)$. Then for plane waves with vacuum wavenumber $k = \omega/c$, Maxwell's equation yields

$$\frac{\mathrm{d}^2\mathcal{E}}{\mathrm{d}x^2} + k^2 n_r^2(x)\mathcal{E} = 0\ . \tag{2.10}$$

Consider now the time independent Schrödinger equation for a particle with energy $E = \hbar^2 k^2/2m$ and subject to a potential $V(x)$

$$\frac{\mathrm{d}^2\psi}{\mathrm{d}x^2} + k^2\left(1 - \frac{V(x)}{E}\right)\psi = 0. \tag{2.11}$$

Comparing the above two equations, we see that in the Maxwell equation, the eigenvalue k^2 multiplies the "potential" term $n_r^2(x)$, whereas in the Schrödinger equation the eigenvalue k^2 is absent in front of the potential $V(x)$. We see that the two equations are identical if we identify

$$n_r^2(x) = 1 - \frac{V(x)}{E} \tag{2.12}$$

We assume here that $n_r^2 > 1$, which implies that in order for this identification between the two equations to hold, we must have $V(x) < 0$. Therefore, by making this connection we see that quantum mechanically the central mirror acts as a potential well. This is why the global odd solutions are lower than the even solutions. Another key difference between the two equations arises when one considers conserved quantities. The wave function ψ must satisfy the normalization condition $\int_{-L_1}^{L_2} |\psi(x)|^2 \mathrm{d}x = 1$. This condition arises from the conservation of probability. The same is not true of the Maxwell wave equation. The discrepancy arises due to the fact that energy is not conserved due to an influx of energy to the system caused by moving the central mirror. As was mentioned above, the electromagnetic energy density is proportional to $\mathcal{E}^2$ and therefore is not conserved.

2.2.3 Mode Approximation

The benefit of using the δ-model is that it allows us to derive analytic results rather easily. We expand Eq. (2.7) about $\Delta L = 0$ and obtain to second order the following expressions for the wavenumbers of the global even and odd modes valid at, and in the vicinity of, the avoided crossings centered at $\Delta L = 0$ (see Appendix D for derivations)

$$k_{n,e} = \frac{2\pi n}{L} + \frac{1}{2\pi n}\frac{1}{\frac{\alpha}{4} + \frac{L}{(2\pi n)^2}} + \frac{2\pi^3 n^3 \alpha \Delta L^2}{L^4} \tag{2.13}$$

$$k_{n,o} = \frac{2\pi n}{L} - \frac{2\pi^3 n^3 \alpha \Delta L^2}{L^4} \,. \tag{2.14}$$

These analytic approximations agree very well with numeric solutions provided one is quite high up in the spectrum (optical regime), but only in the immediate vicinity of an avoided crossing. As one moves away from the avoided crossing, it becomes evident that these approximations breaks down as they do not exhibit the asymptotically linear behavior seen in Fig. 3. A way to remedy this is by fitting the wavenumbers close to an avoided crossing to the functions

$$k_{n,e} = \frac{2\pi n}{L} + \frac{\Delta}{\hbar c} + \frac{1}{\hbar c}\sqrt{\Delta^2 + \gamma\,\Delta L^2} \tag{2.15}$$

$$k_{n,o} = \frac{2\pi n}{L} + \frac{\Delta}{\hbar c} - \frac{1}{\hbar c}\sqrt{\Delta^2 + \gamma\,\Delta L^2} \tag{2.16}$$

because these are the forms given by the Landau-Zener hamiltonian (3.1), as will be explained in Section 3.1. The gap between the wavenumbers of the even and odd global solutions at an avoided crossing is given by $2\Delta/\hbar c$, where for later convenience we have defined Δ as an energy. The parameters γ and Δ can be obtained by matching the Taylor expansions of Eqns (2.15) and (2.16) to Eqns (2.13) and (2.14), respectively. We find

$$\gamma = 2\Delta\,\hbar c\,\frac{2\pi^3 n^3 \alpha}{L^4} \tag{2.17}$$

$$\Delta = \frac{\hbar c}{L}\frac{n\pi}{1 + n^2\pi^2\alpha/L} \,. \tag{2.18}$$

Note that this expression for Δ is valid up to second order in the quantity $\epsilon = kL - 2\pi n$, i.e. the deviation of the solutions from the perfectly localized case. ϵ is small if $\alpha k \gg 1$, which is the case for reasonably reflective mirrors and optical wavenumbers. A comparison between the values of k found from an exact numerical solution of Eq. (2.7), and the approximate analytic solutions given by Eqns (2.15) and (2.16) is included in Fig. 2.2. It is notable that the degeneracy of the localized solutions at $\Delta L = 0$ exactly coincides with the lower branch of the corresponding global solutions at the avoided crossing rather than lying halfway between the two global branches. This is because the lower global branch corresponds to an odd solution in the double cavity. Odd solutions have a

node at the δ-mirror and hence do not see the mirror at all.

2.3 Transfer Ratio

Once the wavenumbers are known, the field amplitudes A_n and B_n for the left and right sides of the common mirror can be calculated. From the continuity condition for the field across the mirror we find that

$$\frac{A_n}{B_n} = -\frac{\sin(k_n L_2)}{\sin(k_n L_1)} = -\frac{\sin[k_n(L-\Delta L)/2]}{\sin[k_n(L+\Delta L)/2]} \ . \tag{2.19}$$

Using this ratio one can construct the global wavemodes inside the cavity. Figure 2.3 shows a series of plots for a pair of wavemodes, illustrating how they swap sides as the common mirror is moved through an avoided crossing. The mirror only needs to be moved by approximately one quarter of a wavelength to achieve the transfer of light from one cavity to the other.

The ratio given by Eq. (2.19) is a key quantity because it is a measure of the degree to which the field is localized on one side or the other, and thus the efficacy of the transfer. In Figure 2.4 we plot A_n/B_n as a function of ΔL, for the case $\alpha/L = 1$. The maxima of the ratio A_n/B_n are located at values of the mirror displacement which are roughly halfway between pairs of avoided crossings. We shall denote these values of the mirror displacement by $\Delta L_{n\star}$. Accordingly, we shall denote the values of the wavenumbers at these points by $k_{n\star}$. In Appendix A, we derive a transcendental equation for $k_{n\star}$ given by:

$$\tan(k_{n\star}L) = -\frac{\alpha k_{n\star} L}{2L+\alpha} \tag{2.20}$$

As can be seen in Figure 2.1, halfway between the avoided crossings the wavenumbers k_n have a linear dependence on ΔL. By inserting a linear ansatz for k_n into Eq. (2.19), we obtain an expression for k_n valid in the neighborhood of $k_{n\star}$

$$k_n \approx k_{n\star} + \frac{k_{n\star}\sin(k_{n\star}L)}{L\sin(k_{n\star}\Delta L_{n\star}) - \Delta L_{n\star}\sin(k_{n\star}L)}(\Delta L - \Delta L_{n\star}) \tag{2.21}$$

where $k_{n\star}$ can be found by taking a linear approximation of Eq. (2.20) to obtain

$$k_{n\star,e/o} = \frac{1}{L}\frac{2\alpha(2\pi n \pm \pi/2)^3 + (8L+4\alpha)(2\pi n \pm \pi/2)}{2\alpha(2\pi n \pm \pi/2)^2 + 4L + 2\alpha} \ . \tag{2.22}$$

Here the plus/minus corresponds to the even/odd wavemodes respectively (See Appendix A for a full derivation). It is important to note that this approximation breaks down when $\alpha \ll L$. The mirror displacement $\Delta L_{n\star}$ is found by solving the transcendental equation (2.7) for ΔL and evaluating it at $k_{n\star}$, i.e.

$$\Delta L_{n\star} = \frac{1}{k_{n\star}} \arccos\left[\frac{2\sin k_{n\star}L}{\alpha k_{n\star}} + \cos k_{n\star}L\right] \tag{2.23}$$

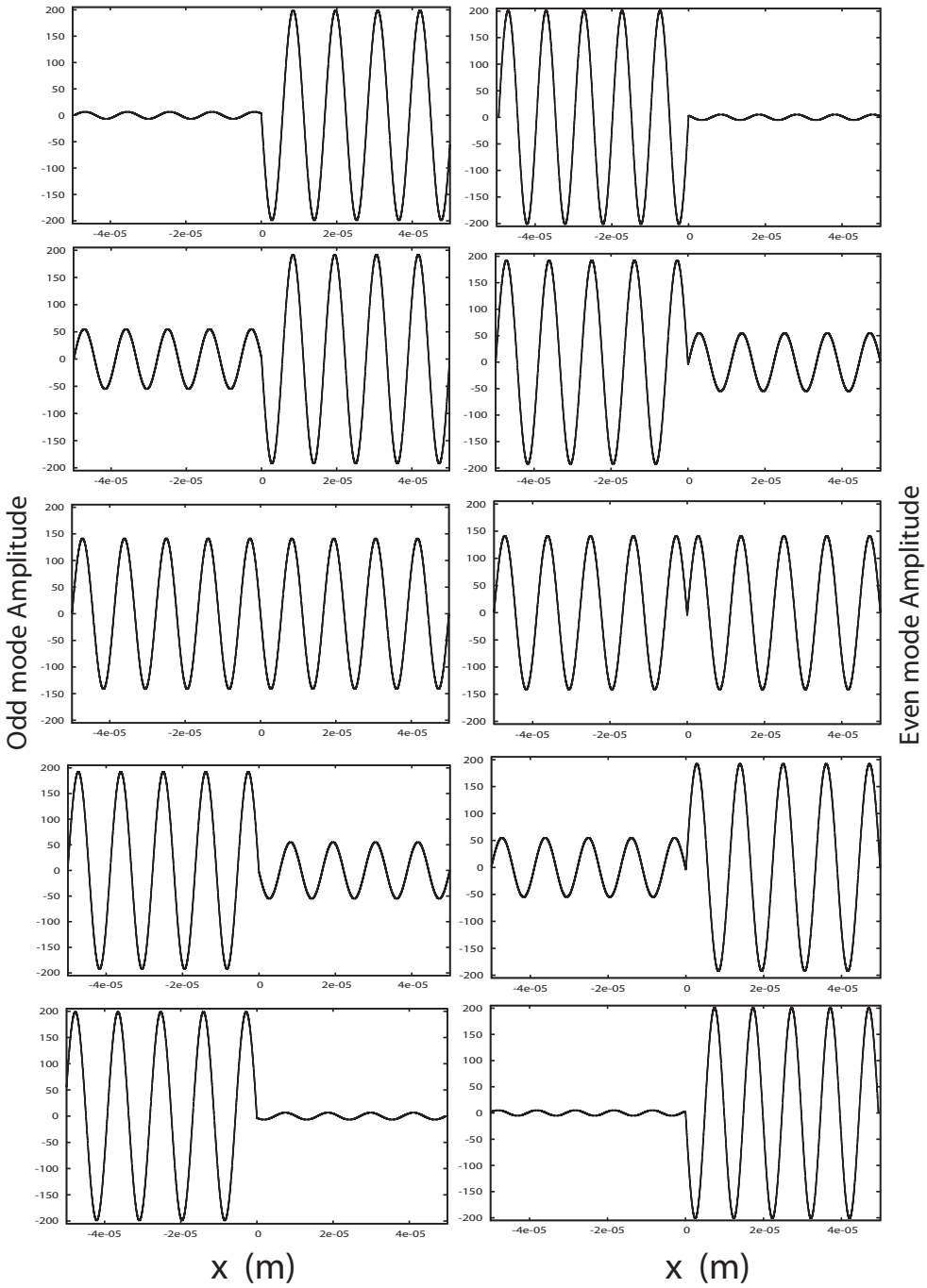

Figure 2.3: This series of plots shows how a pair of global wave modes swap from one side of the double cavity to the other as the common mirror is moved through an avoided crossing. The odd mode $U_{n,\mathrm{odd}}(x)$ plotted as a function of position x is shown in the left column, and the even mode $U_{n,\mathrm{even}}(x)$ is shown in the right column. Each row corresponds to a different value of $\Delta L/L$, which changes from -0.01 to 0.01 from top to bottom. Strictly speaking, the modes only have well defined parity at $\Delta L = 0$, but it is convenient to retain the labels even and odd for $\Delta L \neq 0$. The parameters used to make this figure were $L = 1 \times 10^{-4}$m, $\alpha = 1 \times 10^{-6}$m, and $k \approx 1 \times 10^{8}\mathrm{m}^{-1}$.

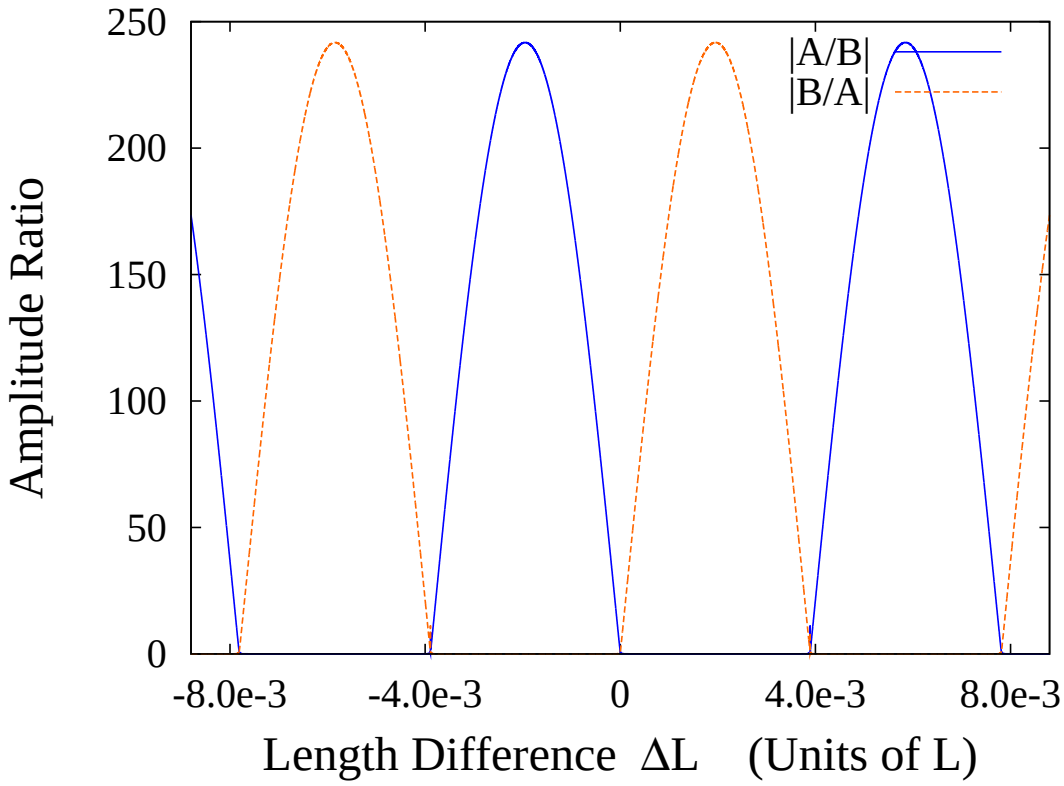

Figure 2.4: The relative amplitudes A_n/B_n and B_n/A_n of the modes as a function of ΔL. The parameters used to make this plot were $L = 1 \times 10^{-4}$m, $\alpha = 0.3 \times 10^{-4}$m, and $n = 128$

Let us now consider the maximum amplitude ratio $\frac{B_{n\star}}{A_{n\star}}$. Near the first maximum point, we expect the numerator to be very near 1, while the denominator is very near 0. We may therefore expand the numerator about $\frac{\pi}{2}$

$$\sin\left(\frac{k_n}{2}(L+\Delta L_n)\right) \approx 1 - \frac{1}{2}\left(\frac{k_n}{2}(L+\Delta L_n) - \frac{\pi}{2} - \pi n\right)^2 \tag{2.24}$$

and expanding the denominator about the nearest zero gives

$$\sin\left(\frac{k_n}{2}(L-\Delta L_n)\right) \approx \frac{1}{2}k_n(L-\Delta L_n) - \pi n \tag{2.25}$$

so that close to a maximum the amplitude ratio can be written

$$\left.\frac{B_n}{A_n}\right|_{\max} \approx \frac{-1+\frac{1}{8}\left(k_{n\star}(L+\Delta L_{n\star}) - (\pi+2n\pi)\right)^2}{\frac{1}{2}k_{n\star}(L-\Delta L_{n\star}) - n\pi}\,. \tag{2.26}$$

We have already found the values of $k_{n\star}$ and $\Delta L_{n\star}$ corresponding to the maximum. We may approximate $\Delta L_{n\star}$ by noting that $k_{n\star}L \approx (2n+1/2)\pi$. This allows us to expand the arccos term in Eq. (2.23) to give

$$\begin{aligned}\Delta L_{n\star} &\approx \frac{1}{k_{n\star}}\left(\frac{\pi}{2} - \frac{2}{\alpha k_{n\star}} + k_{n\star}L - (2n+\frac{1}{2})\pi\right)\\ &= L - \frac{2n\pi}{k_{n\star}} - \frac{2}{\alpha k_{n\star}^2}\end{aligned} \tag{2.27}$$

The maximum amplitude ratio can then be written as

$$\begin{aligned}\left.\frac{B_n}{A_n}\right|_{\max} \approx\ & \frac{\alpha\left(\pi+4n\pi\right)\left(16L+\alpha\left(8+\left(\pi+4n\pi\right)^2\right)\right)}{2L\left(8L+\alpha\left(4+\left(\pi+4n\pi\right)^2\right)\right)}\left[-1+\frac{1}{8}\left(\pi+4n\pi\right.\right.\\ &+ \frac{4L\left(8L+\alpha\left(4+\left(\pi+4n\pi\right)^2\right)\right)}{\alpha\left(\pi+4n\pi\right)\left(16L+\alpha\left(8+\left(\pi+4n\pi\right)^2\right)\right)}\\ &\left.\left.- \frac{\left(\pi+4n\pi\right)\left(16L+\alpha\left(8+\left(\pi+4n\pi\right)^2\right)\right)}{8L+\alpha\left(4+\left(\pi+4n\pi\right)^2\right)}\right)^2\right]\end{aligned} \tag{2.28}$$

We now perform an asymptotic series expansion in the large α limit and keeping only the constant and linear term

$$\left.\frac{B_n}{A_n}\right|_{\max} \approx \frac{2\left(\pi+4n\pi\right)\left(64+80\left(\pi+4n\pi\right)^2+8\left(\pi+4n\pi\right)^4+\left(\pi+4n\pi\right)^6\right)}{\left(4+\left(\pi+4n\pi\right)^2\right)^4}+ \frac{\left(\pi-4n\pi\right)\left(8+\left(\pi+4n\pi\right)^2\right)\left(16+6\left(\pi+4n\pi\right)^2+\left(\pi+4n\pi\right)^4\right)}{2L\left(4+\left(\pi+4n\pi\right)^2\right)^3}\alpha \tag{2.29}$$

In the limit $n \gg 1$ (i.e in the optical regime), this reduces to

$$\left.\frac{B_n}{A_n}\right|_{\max} \approx \frac{1}{2\pi n}+\frac{2\pi n}{L}\alpha \approx \frac{2\pi n}{L}\alpha \tag{2.30}$$

It is now evident that the maximal amplitude swap varies linearly with α (i.e as the reflectivity of the central mirror increases, the transfer ratio increases). However, there is a trade-off due to the fact that as the reflectivity is increased, the gaps at the avoided crossings close up. This implies that slower mirror speeds must be used if the transfer is to be adiabatic, as will be discussed in Section 3.1.

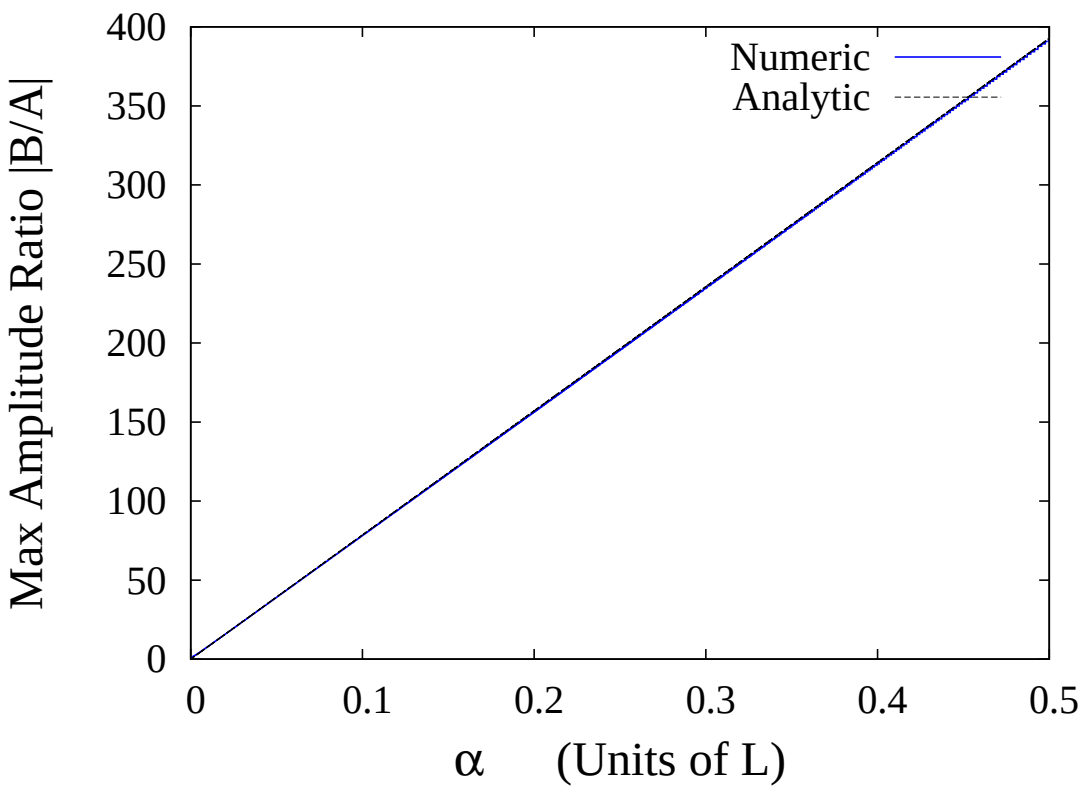

Figure 2.5: The absolute value of the maximum value the relative amplitude B_n/A_n can take as a function of the common mirror parameter α. The exact numerical result is plotted as the blue solid curve, and the approximate analytical result, as given by Eq. (2.30) is plotted as the black dashed curve. Note that the difference between these two curves is hard to discern. We set n=128 to make this plot.

Chapter 3

Quantum Considerations

3.1 Landau-Zener Transitions

The time independent solutions found thus far do not give us the entire picture. The global modes are the instantaneous solutions to Maxwell's wave equation for fixed mirror displacements. If we now suppose that the system started out in a single global mode, then the introduction of time dependence from the moving common mirror will induce transitions to other global modes. By changing the cavity lengths slow enough, we can remain adiabatic (i.e stay in the same eigenstate of the system). In order to solve the dynamics to this problem, and therefore determine whether or not the mode transfer is adiabatic, we map the problem onto that of the closely related Landau-Zener (LZ) problem in quantum mechanics. We may then take advantage of the existing analytic solutions to the problem.

The LZ problem [10, 11, 12] considers a two state quantum system in which the energy separation between the two states is varied linearly in time, passing through a degeneracy at $t = 0$. The two states are coupled by a constant (time-independent) coupling Δ. Stated in this way, the two coupled states are known as the *diabatic* states, and the time-dependent Hamiltonian in the diabatic basis is

$$H_{LZ} = \begin{bmatrix} E(t) & \Delta \\ \Delta & -E(t) \end{bmatrix} \tag{3.1}$$

where the diabatic energies $\pm E(t)$ vary linearly in time $E(t) = \vartheta t/2$. Diagonalizing this Hamiltonian at each instant of time gives the energies $E_\pm$ of the *adiabatic* energies

$$E_\pm(t) = \pm\sqrt{\vartheta^2 t^2/4 + \Delta^2} \tag{3.2}$$

which form an avoided crossing. At the point of closest approach ($t = 0$) the magnitude of the gap between the two adiabatic energies is 2Δ.

At $t = \pm\infty$ the diabatic and adiabatic states coincide, but exchange their associations between $t = -\infty$ and $t = +\infty$, which is the crucial property we need to transfer modes between the two sides of the double cavity. The exact solution of the LZ problem shows that if at $t = -\infty$ the two state system is prepared in one of the two states, then the probability that it has made a transition to the other adiabatic state by $t = +\infty$ is [10, 11, 12]

$$P = \exp(-2\pi\Delta^2/\hbar\vartheta) \ . \tag{3.3}$$

Of course, the LZ problem assumes that there are only two modes present, but due to the exponential suppression in the adiabatic regime of transitions as a function their energy difference, we need only consider a single even and odd pair in the double cavity if we start from a singly occupied mode and move slowly through a single avoided crossing.

Away from the avoided crossings the global modes become localized, each member of a pair localizing on a different side of the common mirror. The larger α is the stronger this localization becomes as was seen in the previous section. The general procedure for the adiabatic transfer of a light mode from one side of the double cavity to the other is now apparent: if the common mirror position is initially set to one side of an avoided crossing (the optimal position is approximately halfway to the next avoided crossing–see Section 2.3) then the localized and global modes approximately coincide and the mode is localized on one side on the common mirror. If the mirror is now slowly translated to the equivalent point on the other side of the avoided crossing, the system will follow the global curve it began on. On the opposite side of the avoided crossing this global mode approximately coincides with the opposite localized mode and so the mode ends up localized on the other side of the common mirror.

At this point, one might be tempted into the following trap. It may seem natural to identify the global wavenumbers with energy as

$$E_+ \equiv \hbar\, c\, k_e \tag{3.4}$$

$$E_- \equiv \hbar\, c\, k_o \tag{3.5}$$

Similarly, ϑ may be extrapolated by noting that away from the avoided crossing the wavenumbers may be assumed to be linear and asymptotic to the diabatic basis. By taking the gradient of the diabatic wavenumber with respect to ΔL, we may identify

$$\vartheta_n \approx 8\pi\hbar c n v/L^2 \ . \tag{3.6}$$

Where we have used the fact that for a perfect central mirror, one has

$$k_n^L \approx \frac{2\pi n}{L}\left(1 - \frac{\triangle L}{L}\right) \tag{3.7}$$

$$k_n^R \approx \frac{2\pi n}{L}\left(1 + \frac{\triangle L}{L}\right) \tag{3.8}$$

for the left and right diabatic wavenumbers respectively. The gap Δ at the avoided crossing can be found from Eqns (2.13) and (2.14). Expressing Δ as an energy, this gives

$$\Delta_n = \frac{\hbar c}{4\pi n}\frac{1}{\frac{\alpha}{4} + \frac{L}{(2\pi n)^2}} \ . \tag{3.9}$$

This temptation, however, is ill founded. In section 2.1 we saw that in the time-independent case, the Maxwell and Schrödinger equations are identical. The problem is that the time evolution of the Maxwell and Schrödinger equations are very different - the Schrödinger equation being first order in time, while the Maxwell wave equation is second order. One might now be inclined to throw in the towel with the LZ approach, but not all is lost. In section (3.2) we derive a first order in time approximation to the Maxwell equation, to which the LZ equation may be applied.

3.2 From Maxwell to Schrödinger

In order to apply the LZ equations, we need to express our system in the proper LZ diabatic basis. It is important remember that the diabatic basis does not in general correspond exactly to the localized modes unless $\alpha \to \infty$ (the LZ diabatic energies must cross halfway between the two adiabatic curves whereas the localized modes do not). To obtain the LZ diabatic modes, we undiagonalize the diabatic representation, using the method presented in Appendix C.

The advantage of working in the diabatic basis, as opposed to the adiabatic basis, is that this allows us to neglect the time dependence of the basis modes, as will be seen below. Consider the time-dependent solution expressed in the diabatic and adiabatic basis. Denoting the diabatic modes as $\phi_L(x)$ and $\phi_R(x)$, we have

$$\mathcal{E}(x,t) = A_L(t)\phi_L(x,t) + A_R(t)\phi_R(x,t) \tag{3.10}$$

$$\mathcal{E}(x,t) = B_e(t)U_e(x,t) + B_o(t)U_o(x,t) \ . \tag{3.11}$$

The time-dependence extends not only to the superposition coefficients but also to the basis modes themselves and this can complicate the treatment. The LZ transition probability (3.3) indicates that changes in the adiabatic superposition coefficients $B_e(t)$ and $B_o(t)$ are exponentially small during a transfer in the adiabatic regime and therefore one cannot ignore changes in the adiabatic modes in comparison to changes in the adiabatic coefficients. This implies that if one were to work in the

adiabatic basis, one would be forced to consider the time dependence of these modes. By contrast, the changes in the diabatic basis in the transition region are typically negligible in comparison to the changes in the coefficients, and so one can take $\phi_L(x)$ and $\phi_R(x)$ to be independent of time [11]. Thus, by working in the diabatic basis we can focus purely on the time-dependence of the coefficients $A_L(t)$ and $A_R(t)$.

The difficulty we now face is that the exact solutions we have found in Chapter 2 pertain to the global modes (equivalent to the adiabatic basis). We shall therefore switch backwards and forwards between the two bases as needed. We begin in the diabatic basis and substitute expression (3.10) for the electric field into the Maxwell wave equation $\partial_x^2\mathcal{E} = \mu_0\varepsilon(x)\partial_t^2\mathcal{E}$. This gives

$$A_L\partial_x^2\phi_L + A_R\partial_x^2\phi_R = \mu_0\varepsilon(x)\big(\ddot{A}_L\phi_L + A_R\ddot{\phi}_R\big) \tag{3.12}$$

where the dots indicate time derivatives. We shall tackle the left and right hand sides of this equation individually.

To simplify the left hand side we substitute the expansions (C.6) and (C.7) of the localized modes in terms of the global modes and then make use of the fact that the global solutions, being eigenmodes of the system, satisfy

$$\partial_x^2 U_e = -\mu_0\varepsilon(x)\omega_e^2 U_e \tag{3.13}$$

$$\partial_x^2 U_o = -\mu_0\varepsilon(x)\omega_o^2 U_o \tag{3.14}$$

to give

$$\partial_x^2\phi_L = -\mu_0\varepsilon(x)\left(-\sin(\theta)\omega_e^2 U_e + \cos(\theta)\omega_o^2 U_o\right) \tag{3.15}$$

$$\partial_x^2\phi_R = -\mu_0\varepsilon(x)\left(\cos(\theta)\omega_e^2 U_e + \sin(\theta)\omega_o^2 U_o\right) \ . \tag{3.16}$$

Now that we have made use of the exact results for the global modes we can go back to the diabatic basis by using (C.8) and (C.9) to obtain

$$\begin{aligned}\partial_x^2\phi_L &= -\mu_0\varepsilon(x)\Big\{\phi_L\big[\sin^2(\theta)\omega_e^2 + \cos^2(\theta)\omega_o^2\big] \\ &+ \phi_R\big[\sin(\theta)\cos(\theta)\omega_o^2 - \sin(\theta)\cos(\theta)\omega_e^2\big]\Big\} \qquad (3.17)\\ \partial_x^2\phi_R &= -\mu_0\varepsilon(x)\Big\{\phi_R\big[\cos^2(\theta)\omega_e^2 + \sin^2(\theta)\omega_o^2\big] \\ &+ \phi_L\big[\sin(\theta)\cos(\theta)\omega_o^2 - \sin(\theta)\cos(\theta)\omega_e^2\big]\Big\} \ . \qquad (3.18)\end{aligned}$$

In order to explicitly express the adiabatic transfer problem in LZ form we let

$$\omega_e = \sqrt{E^2+\Delta^2}/\hbar + \omega_{\rm av} \tag{3.19}$$

$$\omega_o = -\sqrt{E^2+\Delta^2}/\hbar + \omega_{\rm av} \ . \tag{3.20}$$

In these equations $\pm E/\hbar$ are the frequencies of the diabatic modes, as discussed in Appendix C. Indeed, Eqns (3.19) and (3.20) can be viewed as a way of defining the diabatic modes, the adiabatic (global) modes with frequencies ω_e and ω_o being already known from solving of the transcendental equation (2.6). We have also introduced $\omega_{\rm av}$ which is the average frequency of the even and odd modes

$$\omega_{\rm av} = \frac{\omega_e + \omega_o}{2} \tag{3.21}$$

and takes account of the fact that the avoided crossings are not located at frequency $E/\hbar = 0$, but are in fact up in the optical spectrum. These definitions can be combined with expressions (C.4) and (C.5) for $\cos(\theta)$ and $\sin(\theta)$ in terms of the diabatic variables to give

$$\sin(\theta)\cos(\theta)\left(\omega_o^2 - \omega_e^2\right) = 2\Delta\omega_{\rm av} \tag{3.22}$$

which is one of the combinations appearing in (3.17) and (3.18). In a similar fashion we find the other combinations to be given by

$$\sin^2(\theta)\omega_e^2 + \cos^2(\theta)\omega_o^2 = (E/\hbar - \omega_{\rm av})^2 + \Delta^2/\hbar^2 \tag{3.23}$$

$$\cos^2(\theta)\omega_e^2 + \sin^2(\theta)\omega_o^2 = (E/\hbar + \omega_{\rm av})^2 + \Delta^2/\hbar^2 \ . \tag{3.24}$$

Putting all this together we arrive at the following expression for the left hand side of Eq. (3.12)

$$\begin{aligned} &-\mu_0\varepsilon(x)\big[A_L\phi_R 2\Delta\omega_{\rm av} + A_L\phi_L\{(E/\hbar-\omega_{\rm av})^2 + \Delta^2/\hbar^2\} \\ &+A_R\phi_R\{(E/\hbar+\omega_{\rm av})^2 + \Delta^2/\hbar^2\} + A_R\phi_L 2\Delta\omega_{\rm av}\big] \ . \end{aligned} \tag{3.25}$$

In order to treat the right hand side of Eq. (3.12), we remove the fast time evolution associated with the stationary solutions by defining

$$A_{L/R}(t) \equiv \widetilde{A}_{L/R}(t)\exp\left[-i\int_0^t \beta_{L/R}(t')\mathrm{d}t'\right] \ . \tag{3.26}$$

where

$$\beta_{L/R}(t) = \sqrt{(E(t)/\hbar \mp \omega_{\rm av})^2 + \Delta^2/\hbar^2} \ . \tag{3.27}$$

Time derivatives of $A_{L/R}(t)$ then give rise to the terms

$$\begin{aligned}\ddot{A}_{L/R} &= \left(\ddot{\tilde{A}}_{L/R} - 2i\beta_{L/R}\dot{\tilde{A}}_{L/R} - i\dot{\beta}_{L/R}\tilde{A}_{L/R} - \beta_{L/R}^2\tilde{A}_{L/R}\right) \\ &\quad \times \exp\left[-i\int_0^t \beta_{L/R}(t')\mathrm{d}t'\right] . \end{aligned} \tag{3.28}$$

By virtue of the fact that β_L and β_R are so much greater than all the other frequencies in the problem ($\beta_{L/R} \simeq \omega_{\mathrm{av}}$ which is taken to be an optical frequency of order $10^{15}\mathrm{s}^{-1}$), we can neglect the first and third terms on the right hand side of Eq. (3.28). Inserting the remaining terms into the right hand side of Eq. (3.12), and setting this equal to the left hand side as given by Eq. (3.25), we obtain a first order in time approximation to Maxwell's wave equation. Multiplying through by $\varepsilon(x)\phi_L(x)$ or $\varepsilon(x)\phi_R(x)$ and integrating over space in order to make use of the orthogonality conditions (C.10) and (C.11), we can pick out the coupled equations of motion for the amplitudes

$$i\frac{\mathrm{d}\tilde{A}_{L/R}}{\mathrm{d}t} = \frac{\omega_{\mathrm{av}}\Delta}{\hbar\beta_{L/R}}\tilde{A}_{R/L}\exp\left[i\int_0^t(\beta_{L/R} - \beta_{R/L})\mathrm{d}t'\right] . \tag{3.29}$$

These equations can be further simplified by noting that

$$\beta_{L/R} = \omega_{\mathrm{av}}\left(1 \mp \frac{E}{\hbar\omega_{\mathrm{av}}} + \frac{1}{2}\frac{\Delta^2}{\hbar^2\omega_{\mathrm{av}}^2} + \ldots\right) \tag{3.30}$$

and

$$\beta_R - \beta_L = 2E(1 - \frac{1}{2}\frac{\Delta^2}{\hbar^2\omega_{\mathrm{av}}^2} + \ldots) \tag{3.31}$$

and truncating each of these expansions at their first term. In this way we arrive at

$$i\begin{pmatrix}\dot{\tilde{A}}_L \\ \dot{\tilde{A}}_R\end{pmatrix} = \begin{pmatrix} 0 & \frac{\Delta}{\hbar}\mathrm{e}^{-2i\int(E/\hbar)dt'} \\ \frac{\Delta}{\hbar}\mathrm{e}^{2i\int(E/\hbar)dt'} & 0 \end{pmatrix}\begin{pmatrix}\tilde{A}_L \\ \tilde{A}_R\end{pmatrix} \tag{3.32}$$

We have therefore succeeded in mapping the Maxwell wave equation onto the time-dependent Schrödinger equation. We are now justified in applying the LZ result (3.3) to the problem of a slowly moving mirror in a double cavity.

3.3 Quantization

We have seen how a classical treatment of the optomechanical dynamics reduces to a Schrodinger equation in the regime of interest. We now instead wish to begin with the second-quantized Hamiltonian for the double cavity, and show that our formalism gives a second-quantized version of the LZ Hamiltonian. Note that this treatment is only valid for the static mirror case. The even and odd modes constitute the normal modes, which allows us to write the Hamiltonian as (setting $\hbar = 1$)

$$\hat{H} = \omega_e a_e^\dagger a_e + \omega_o a_o^\dagger a_o \tag{3.33}$$

Here a_e is the annihilation operator for a photon in the even mode, and a_o is the annihilation operator for a photon in the odd mode. We transform this into the diabatic basis by letting

$$\begin{aligned} a_e &= \cos\theta\ b_R - \sin\theta\ b_L \\ a_o &= \sin\theta\ b_R + \cos\theta\ b_L. \end{aligned} \tag{3.34}$$

where we may view b_R and b_L as right cavity and left cavity annihilation operators respectively. We then find that

$$\begin{aligned} & \omega_e a_e^\dagger a_e + \omega_o a_o^\dagger a_o = (\omega_e \cos^2\theta + \omega_o \sin^2\theta) b_R^\dagger b_R \\ + & (\omega_e \sin^2\theta + \omega_o \cos^2\theta) b_L^\dagger b_L \\ + & \cos\theta \sin\theta (\omega_o - \omega_e) b_R^\dagger b_L \\ + & \cos\theta \sin\theta (\omega_o - \omega_e) b_L^\dagger b_R \end{aligned} \tag{3.35}$$

Using expressions derived for $\cos\theta$ and $\sin\theta$ given by Eqns C.4 and C.5, along with those for ω_e and ω_o given by Eqns (3.19) and (3.20), we arrive at the second quantized hamiltonian in the diabatic basis

$$H = (\hbar\omega_{\text{av}} + E) a_R^\dagger a_R + (\hbar\omega_{\text{av}} - E) a_L^\dagger a_L + \Delta(a_R^\dagger a_L + a_L^\dagger a_R) \tag{3.36}$$

Therefore we see that we may indeed write the Hamiltonian in LZ form using left cavity and right cavity creation/annihilation operators for photons.

Chapter 4

Beyond the δ-function model

4.1 Finite Width Mirror

We now investigate the finite mirror system and compare solutions to that of the δ-function model. The finite model gives a more realistic description of the mirror, while the δ-function model is mathematically more tractable. We compare the eigenvalue structure of the two models and look at their reflection and transmission coefficients. Our main goal in this section is to examine how well the δ-function model reproduces the results of the finite model.

We model the finite barrier as a uniform slab of dielectric material with finite width $2M$. The corresponding permeability function is given by

$$\epsilon(x) = \begin{cases} \epsilon_0\,(1+H) & -M < x < M \\ \epsilon_0 & -L_1 < x < -M \ and \ M < x < L_2 \\ \infty & elsewhere \end{cases}$$

where $n_r = \sqrt{1+H}$ is the index of refraction inside the slab.

Imposing the boundary condition $U_n(-L_1) = U_n(L_2) = 0$, the eigenmode can be written as:

$$U_n(x) = \begin{cases} A\sin\left[k(x+L_1)\right] & -L_1 < x < -M \\ B\sin\left(n_r kx + \phi_1\right) & -M < x < M \\ C\sin\left[k(x-L_2)\right] & M < x < L_2 \end{cases}$$

From the continuity of the eigenmode and it's first derivative, we find an equation for the allowed

wavenumbers

$$
\begin{aligned}
& n_r^2 \sin(2n_r kM) \sin\left[k\left(\frac{L}{2} - M + \frac{\Delta L}{2}\right)\right] \times \\
& \sin\left[k\left(\frac{L}{2} - M - \frac{\Delta L}{2}\right)\right] \\
& + n_r \cos(2n_r kM) \sin[k(L-2M)] \\
& + \sin(2n_r kM) \cos\left[k\left(\frac{L}{2} - M + \frac{\Delta L}{2}\right)\right] \times \\
& \cos\left[k\left(\frac{L}{2} - M - \frac{\Delta L}{2}\right)\right] = 0\,.
\end{aligned}
\tag{4.1}
$$

It is important to note that the mirror resonances occur when $2Mkn_r = l\pi$, where $l = 1, 2, 3, \ldots$. Figure (4.2) shows the "vertical" avoided crossings created near one such resonance. We now wish to understand under what conditions, the finite barrier (FB) model converges to the δ-function model. To understand this, we compare the reflection coefficient for the FB model and the δ-function model (see Appendix B for a derivation).

$$
R_{FB} = \frac{1}{1 + \frac{4n^2}{(n^2-1)^2 \sin^2(2n\bar{k}\bar{M})}} \tag{4.2}
$$

$$
R_{\delta} = \frac{1}{1 + \frac{4}{\bar{k}^2 \bar{\alpha}^2}} \tag{4.3}
$$

give the corresponding finite and delta reflection coefficients.

If we take the limits in which $M \to 0$ and $n_r \to \infty$, while we hold $n_r^2 M$ constant in the process, we find the relationship between the two models is given by $\alpha = 2Mn_r^2$

Figures (4.1) and (4.2) show wavenumbers for both the delta and finite mirror far from a resonance as well as near a resonance condition.

It is clear from figure (4.2) that near a resonance of the central mirror, the finite mirror and δ will not agree. This disagreement is due to the electromagnetic field being trapped in the common mirror. It is however quite interesting to note that even in the case where one is far from a resonance of the central mirror (4.1), we still do not see perfect matching. This may at first come as a surprise as we had just finished showing that we may match reflectivities of both the finite and δ mirrors. If we then adjust the length of the finite cavity to match that of the δ cavity by increasing the length of both the left and right cavities by M, then both models should yield identical wave dynamics. However, one must also consider the phase of the transmission function for the common mirror. In appendix(B) it is shown that by matching the reflection or transmission probabilities of the two models, we are not infact matching the phase of the transmitted waves. This leads to perturbations in the wavenumbers and accounts for the variability between the delta and finite barrier models. All is not lost however, as the two models agree very well in certain regions. In order to find these

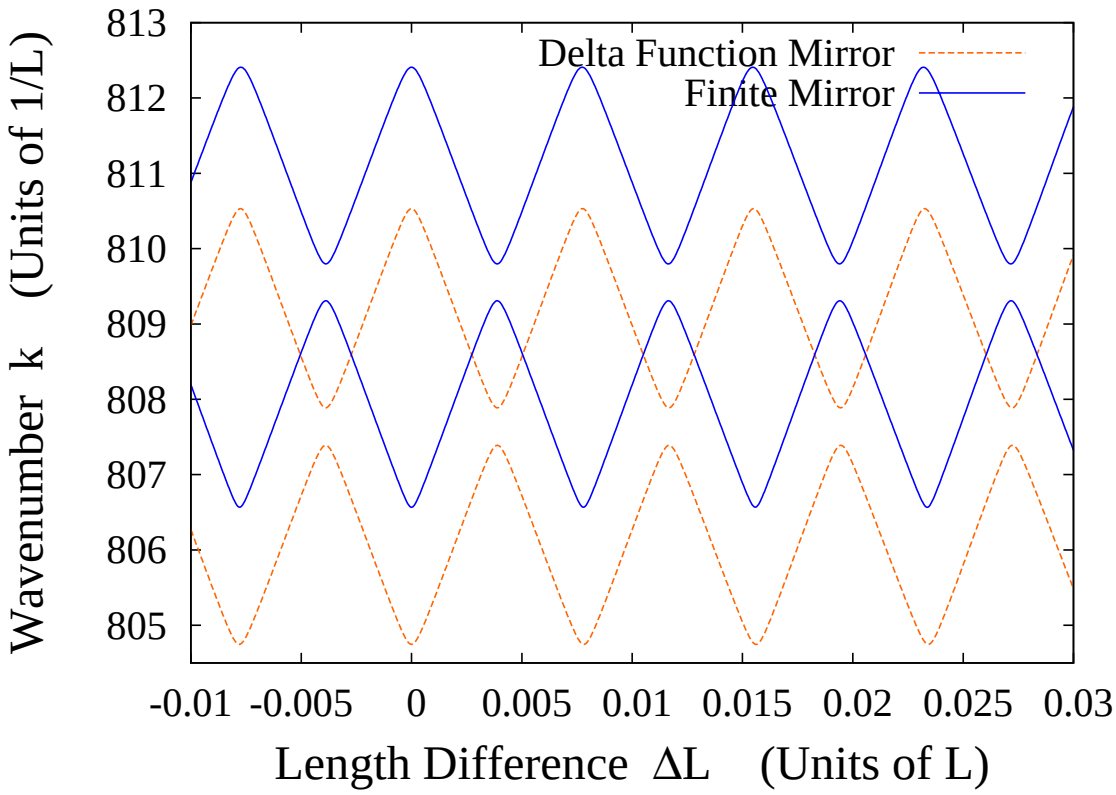

Figure 4.1: Comparison between the wavenumber structure produced by a mirror of width $2M$ (solid blue curves) and the δ-mirror (dashed red curves) inside a double cavity. This plot is for the case when we are far from a mirror resonance. In order to make the comparison we matched the transmission probabilities T for each mirror over the relevant range of wavenumbers as best we could (see Fig. 4.3). Up to a relative vertical shift, the agreement is very good, including the magnitude of the gap 2Δ at the avoided crossings. In the calculation for the δ-function mirror we set $\alpha/(L-2M) = 0.01003$. In the finite mirror calculation we set $M/(L-2M) = 0.001334$ and $2n_r^2 M/(L-2M) = 0.1707$. Note that to make this plot clearer we have only included the wavenumbers for a single pair of modes in each case.

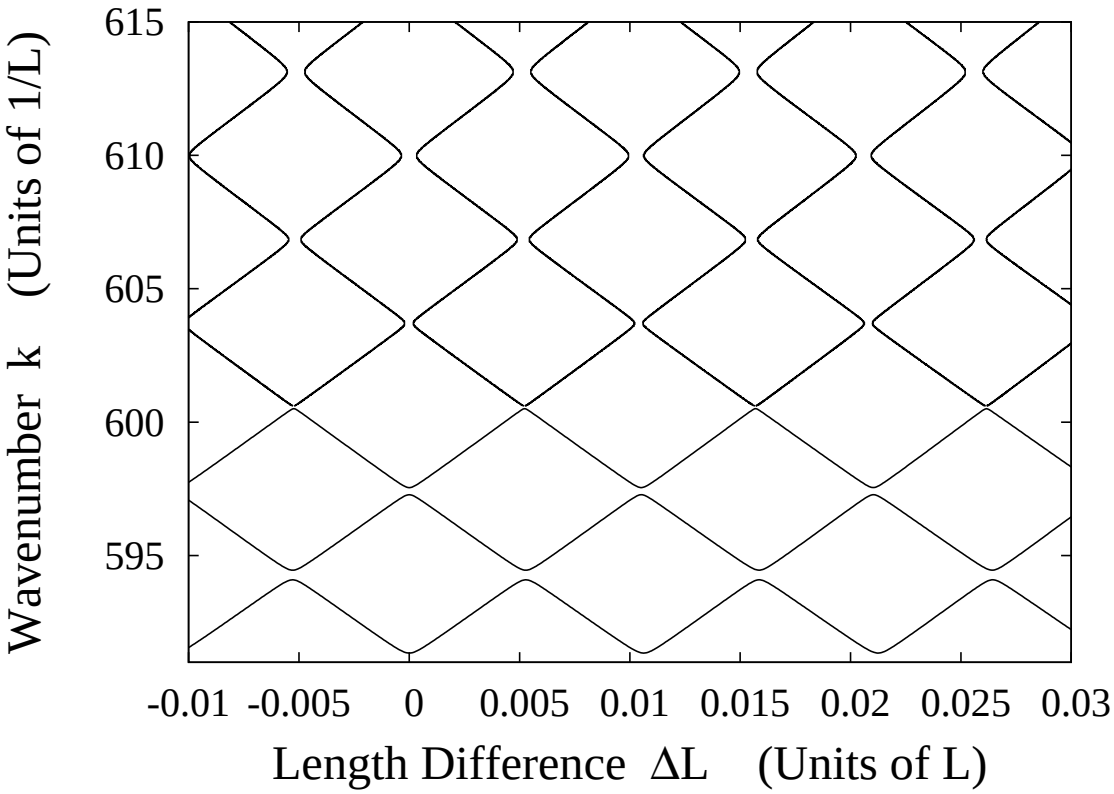

Figure 4.2: The wavenumber structure produced by a mirror of width $2M$ inside a double cavity. This plot includes wavenumbers for which there is a mirror resonance. At the bottom we see the familiar avoided crossing structure which couples even and odd modes with the same index n, but for higher wavenumbers we pass into resonance and the structure changes to one where there are vertical avoided crossings that allow for the possibility of adiabatically coupling localized cavity modes with different values of the index m. The parameters used to make this plot were M/(L-2M)=0.0005005, and $2n_r^2 M/(L-2M) = 0.01001$.

regime, we must match the reflectivities of the two models in such a way that it is insensitive to changes in the wavenumber k_n. The ideal matching occurs when the finite mirror reflectivity R_{FB} is away from a resonance, and at a minimum point so that there is no first order change with respect to k_n. This requires us to find the stationary points of R_{FB}.

$$\frac{dR_{FB}}{dk_n} = -\left[1 + \frac{4n^2}{(n^2-1)^2 sin^2(2nkM)}\right]^{-2} \left[\frac{8n^3 M(n^2-1)^2 sin(4nkM)}{L(n^2-1)^4 sin^4(2nkM)}\right] = 0$$

$$\Rightarrow \quad sin(2n\bar{k}\bar{M}) = 0$$

$$\Rightarrow \quad \bar{k} = \frac{z\pi}{4n\bar{M}} \qquad z\epsilon\mathbb{Z}$$

However, only odd z are of interest as the even multiples give the resonance points. Figure 4.3 shows a plot comparing transmission probabilities for both models as a function of the wavenumber k. The matching occurs at a minimum point of the finite transmission curve.

4.2 Experimental realizability

We now turn to the problem of realizing an adiabatic transfer in practice. The key challenge is to achieve adiabatic transfer between cavities before light leaks out of the system. This leakage occurs due to the fact that the end mirrors are not perfectly reflecting in practice. Let us consider a double cavity of length $L = 10^{-4}$(m) comprised of 2 outer mirrors with a finesse $F_1 = 10^6$ [16, 17, 18, 19] and an inner mirror with $\alpha = 0.3L$. The speed at which the central mirror moves becomes an important parameter to consider due to losses out of the cavity. The current fastest piezo-electric motors obtain velocities of 0.8m/s [15]. In order to amplify the transfer rate, we may rig the system so that all 3 mirrors now move instead of just the central mirror. As only the difference in cavity length $\Delta L = L_1 - L_2$ is relevant, this allows us to effectively double the central mirror speed. To see why, consider the following. Let x_1, x_2, and x_3 be the positions of the left mirror, central mirror, and right mirror respectively. The length of the left cavity is given by

$$L_{left}(t) = (x_1 - 0.8t) - (x_2 + 0.8t) = L_1 - 1.6t \tag{4.4}$$

Likewise,the right cavity length is

$$L_{right}(t) = (x_2 + 0.8t) - (x_3 - 0.8t) = L_2 + 1.6t \tag{4.5}$$

Therefore we see that

$$\Delta L(t) = L_{left}(t) - L_{right}(t) = L_1 - L_2 - 3.2t = \Delta L - 3.2t \tag{4.6}$$

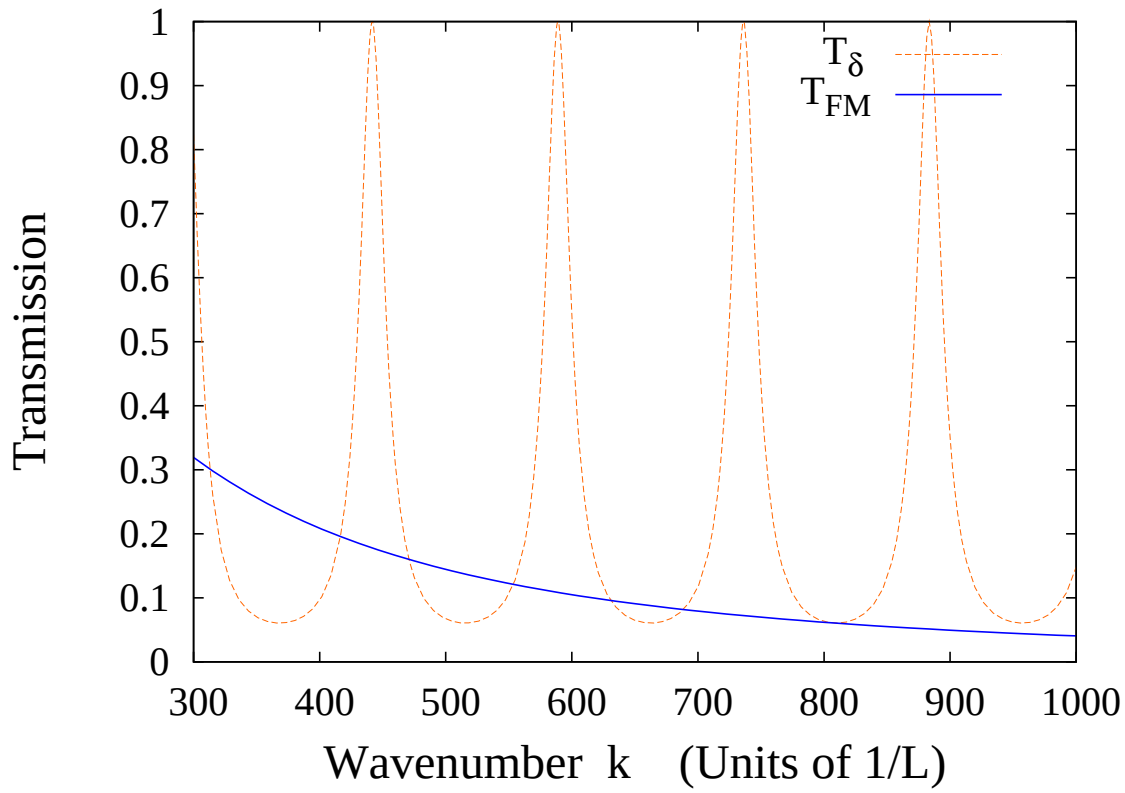

Figure 4.3: A comparison of the transmission probability T for the finite and δ-function mirrors, as given by Eqns (B.8) and (B.16), respectively . The resonances of the finite mirror occur at the peaks of its transmission function. Over the range of k shown in Fig. 4.1, the two curves intersect near a minimum of the finite barrier transmission and so are in close agreement. The parameters used to make this plot are given in the caption of Fig. 4.1.

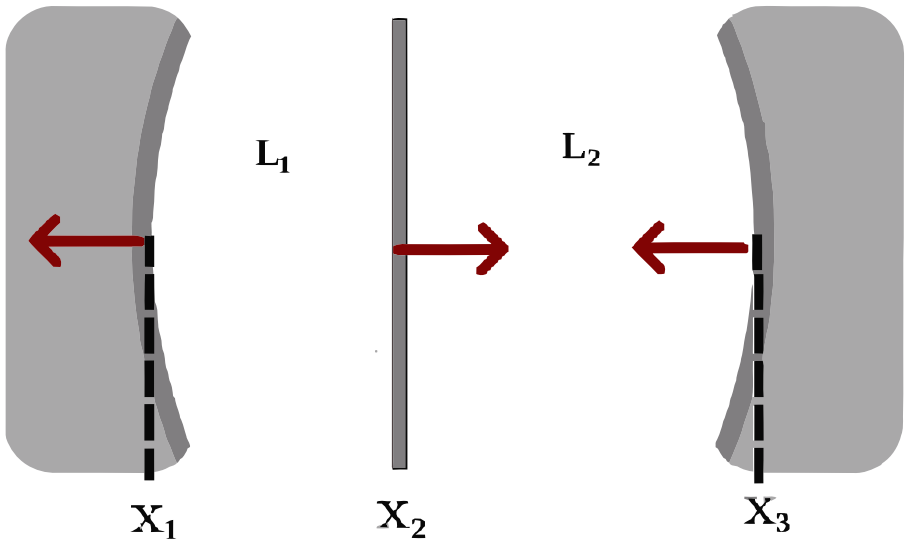

Figure 4.4: By moving all 3 mirrors, it is possible to enhance the speed at which interference occurs, and thereby reduce losses

which translates to an effective mirror velocity of 1.6m/s.

The question of how much one must change ΔL in order to obtain a transfer will now be addressed. The problem becomes an optimization problem between obtaining a maximal amplitude transfer from left localization to right localization, and minimizing the cavity losses due to experimental limitations in central mirror speed. We consider light in the wavelength range of $780nm$, and examine the amplitude ratio plot for a wavemode near an avoided crossing at $\Delta L = 0$.

From the plot, it's clear that one may obtain an amplitude transfer ratio of 10:1 with a relative displacement $\Delta L = 0.00005L$. The time it takes to displace the mirrors by this much is $t = 3.2 \times 10^{-9}s$. The losses obtained in this time may be found by using $E(t) = E_o e^{-\kappa t}$, where $\kappa = c\pi/2dF$. Here $d = 0.0001m$, and $F = 10^6$. Using these parameters we obtain $\kappa = 4.7 \times 10^6$, and find that we have approximately a 1.5% loss during this interval. It is now an opportune time to emphasize the importance of the central mirror reflectivity. The higher the reflectivity, the steeper the amplitude ratio curve becomes, and hence, the shorter the distance one must traverse in order to hit a desired transfer ratio. The caveat for using such a high finesse central mirror is that the avoided crossing distances shrink the higher the mirror reflectivity. Thus it becomes important to make sure that at the transfer rates being used, the cavity swapping remains adiabatic. Using the same parameters as above, we calculate the probability of remaining adiabatic as one transfers photons from one side to

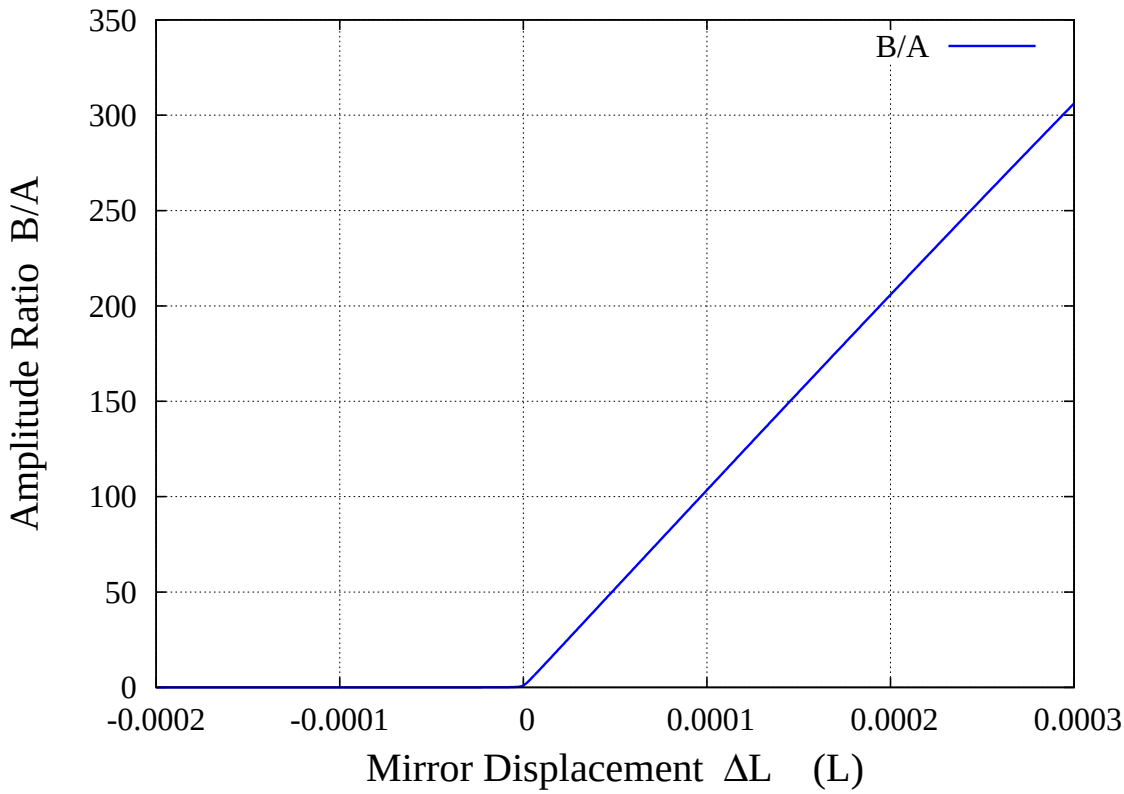

Figure 4.5: A zoomed in plot of the relative amplitudes against the displacement ΔL. From the plot, it's clear that one need only very small perturbations about equilibrium in order to acheive large amplitude transfers. Here $\alpha = 0.3L$ and $n = 128$

the other.

The Lanau-Zener transition probability is given by $P = \exp(\frac{-2\pi\Delta^2}{\hbar\vartheta})$. In this case one finds $\Delta \approx 120.0\hbar c$, and $\vartheta \approx 5.1 \times 10^{11}\hbar c$. Substituting this in, one finds that the probability of making a transition is effectively zero, and the transfer will be adiabatic with almost certainty.

Chapter 5

Future Work

Our efforts thus far have been focused on a classical treatment of the dynamics of electromagnetic waves in a double cavity. We have seen that the finite barrier model introduced some interesting behavior, such as horizontal avoided crossings (Figure 4.2) which occur near the central mirror resonance. This behavior is not well understood, and requires further investigation. The next important step is to extend the model to a 3-cavity system. This more complicated toy model would be representative of the real system of interest, which is that of two semi-isolated cavities joined by an optical fiber. This poses an entirely new set of problems, as one would now be in a situation in which the modes are closely spaced (as the central cavity length may be significantly larger than the other two cavities). It might then be difficult to isolate a single mode in the fiber. Instead, we would be in a superposition of many such states which may wreck havoc on our ability to efficiently transfer light between the end cavities. A possible approach would be to use a STIRAP like technique [5] in which the intermediate state (i.e the state in the central cavity) would never be occupied, thereby eliminating the trouble caused by this region. The final step would then to be introduce atoms into the cavities and allow them to interact with the quantized electromagnetic field. With atoms in place, we would have a simple quantum network, ready to be tested by experiments. The parameter regime we have focused on in this paper corresponded to the optical regime. However, the basic idea of adiabatic transfer of electromagnetic fields between cavities can also be applied at other wavelengths, e.g. microwave, which is relevant both to Maser type set-ups [21], as well as to the new field of circuit QED where superconducting qubits play the role of "artificial atoms" in microwave resonators [22].

Chapter 6

Conclusion

We have seen that optomechanical systems in which the cavity mode structure is varied dynamically by externally shifting a common mirror brings an interesting new approach to the problem of photon transfer in quantum networks. The system allows for robust and efficient transfer of light from one cavity to another, in a non-time sensitive manner. The system also benefits from it's simplicity and the ability to produce analytic results. We were able to derive expressions for the wavenumber approximations near avoided crossings, as well as at the maximal amplitude transfer points. This in turn allowed for analytic expressions for the maximal amplitude transfer between the left and right cavities given by equation (2.30). By showing that Maxwell's equations may reduce to a Schrödinger equation in the optical regime, we were able to apply results from Lanau-Zener to our classical problem and obtain an expression for the transition probability of jumping between wavenumbers during a photon transfer (3.3). The δ model was shown to do an excellent job at reproducing the finite barrier dynamics so long as one stays away from the common mirror resonance. One of shortcomings of the setup however, is that it is inherently only suitable for short networking. This is due to the fact that we must be able to isolate energy levels, and therefore need the separation between the modes to be appreciable.

Appendix A

Derivation of maximal amplitude wavenumber approximation

Let us now derive the values of k_n and $\triangle L$ at the maximum point of $\frac{A_n}{B_n}$. We begin by differentiating the amplitude ratio (2.19) with respect to $\triangle L$.

$$\begin{aligned}\frac{d}{d\triangle L}\left(\frac{A_n}{B_n}\right) &= \frac{-\sin\left(\frac{k_n}{2}(L+\triangle L)\right)\cos\left(\frac{k_n}{2}(L-\triangle L)\right)\left[\frac{\dot{k}_n}{2}(L-\triangle L)-\frac{k_n}{2}\right]}{\sin^2\left(\frac{k_n}{2}(L+\triangle L)\right)} \\ &+ \frac{\sin\left(\frac{k_n}{2}(L-\triangle L)\right)\cos\left(\frac{k_n}{2}(L+\triangle L)\right)\left[\frac{\dot{k}_n}{2}(L+\triangle L)+\frac{k_n}{2}\right]}{\sin^2\left(\frac{k_n}{2}(L+\triangle L)\right)} \end{aligned} \tag{A.1}$$

At a critical point, we require this to be zero. Solving for $\dot{k}_n$ yields

$$\dot{k}_n = \frac{k_n \sin(k_n L)}{L\sin(k_n\triangle L) - \triangle L \sin(k_n L)} \tag{A.2}$$

Going back to the transcendental equation (2.7) for the eigen-wavenumbers, we may differentiate with respect to $\triangle L$ in order to obtain an expression for $\dot{k}_n$. Performing the differentiation and rearranging, we obtain:

$$\dot{k}_n = \frac{k_n \sin\left(k_n\triangle L\right)}{L\sin\left(k_n L\right) - \triangle L\sin\left(k_n\triangle L\right) - \frac{2L}{\alpha}\left(\frac{\cos(k_n L)}{k_n} - \frac{\sin(k_n L)}{k_n^2 L}\right)} \tag{A.3}$$

Equating equation (A.2) with (A.3)

$$
\begin{aligned}
& L^2 \sin^2(k_n L) - L\triangle L \sin(k_n \triangle L)\sin(k_n L) - \frac{2L^2}{\alpha}\left(\frac{\cos(k_n L)\sin(k_n L)}{k_n} - \frac{\sin^2(k_n L)}{k_n^2 L}\right) \\
= \; & L^2 \sin^2(k_n \triangle L) - L\triangle L \sin(k_n L)\sin(k_n \triangle L) \qquad \text{(A.4)}
\end{aligned}
$$

rearranging this

$$
\sin^2(k_n L) - \frac{2}{\alpha}\left(\frac{\cos(k_n L)\sin(k_n L)}{k_n} - \frac{\sin^2(k_n L)}{k_n^2 L}\right) - 1 + \cos^2(k_n \triangle L) = 0 \qquad \text{(A.5)}
$$

Substituting in the transcendental wavenumber equation (2.7) for $\cos(k_n \triangle L)$ then gives us

$$
2\cos(k_n L) + \frac{\sin(k_n L)}{k_n L}\left(\frac{4L + 2\alpha}{\alpha}\right) = 0 \qquad \text{(A.6)}
$$

which we may rewrite as

$$
\tan(k_{n\star}\Delta L_{n\star}) = -\frac{\alpha k_{n\star}\Delta L_{n\star}}{2\Delta L_{n\star} + \alpha} \qquad \text{(A.7)}
$$

The maximum value occurs very near the midpoint between avoided crossings (i.e when $k_n \approx 2\pi n \pm \pi/2$ for even and odd modes respectively). In this region, k_n is very nearly linear, and so we expand the cosine and sinc functions in (A.6) to first order around this point

$$
-2\left(k_{n\star}L - (2\pi n \pm \pi/2)\right) + \frac{4L + 2\alpha}{\alpha}\left(\frac{1}{2\pi n \pm \pi/2} - \frac{1}{(2\pi n \pm \pi/2)^2}\left[k_{n\star}L - (2\pi n \pm \pi/2)\right]\right) = 0 \qquad \text{(A.8)}
$$

$$
k_{n\star}L = \frac{2\alpha(2\pi n \pm \pi/2)^3 + (8L + 4\alpha)(2\pi n \pm \pi/2)}{2\alpha(2\pi n \pm \pi/2)^2 + 4L + 2\alpha} \qquad \text{(A.9)}
$$

Note that in this derivation, the n value is the pair number. To obtain the corresponding $\triangle L$ value, we rearrange the trascendental wavenumber equation (2.7) to obtain:

$$
\triangle L_{n\star} = \frac{1}{k_{n\star}}\cos^{-1}\left(\frac{2}{\alpha}\frac{\sin(k_{n\star}L)}{k_{n\star}} + \cos(k_{n\star}L)\right) \qquad \text{(A.10)}
$$

We may approximate $\triangle L_{n\star}$ by noting that $k_{n\star}L \approx (2n + \frac{1}{2})\pi$. We are then able to take a first order expansion

$$\begin{aligned}
\triangle L_{n\star} &= \frac{1}{k_{n\star}} \cos^{-1}\left(\frac{2}{\alpha}\frac{\sin(k_{n\star}L)}{k_{n\star}} + \cos(k_{n\star}L)\right) \\
&\approx \frac{1}{k_{n\star}}\left(\frac{\pi}{2} - \frac{2}{\alpha k_{n\star}} + k_{n\star}L - (2n+\frac{1}{2})\pi\right) \\
&= L - \frac{2n\pi}{k_{n\star}} - \frac{2}{\alpha k_{n\star}^2} \qquad \text{(A.11)}
\end{aligned}$$

Appendix B

Transmission and Reflection for lossless dielectric mirrors

Let us examine a possible explanation for where the variability between the finite model and the delta model may originate from. Let us consider the transmission functions for both models. This will also give the ability to relate the parameter α to the reflectivity R and wavenumber k_n. Suppose we send a plane wave towards our central delta mirror from the left. The plane wave will then take the form:

$$E_n(x) = \begin{cases} A_{right}e^{ik_n x} + A_{left}e^{-ik_n x} & x < 0 \\ B_{right}e^{ik_n x} + B_{left}e^{-ik_n x} & x > 0 \end{cases} \tag{B.1}$$

Imposing continuity of the wave at $x = 0$ gives:

$$E_n(0) = A_r + A_l = B_r + B_l \tag{B.2}$$

Integrating equation Eq. (2.2) around a $\delta - neighborhood$ of $x = 0$ yields:

$$\frac{i}{k_n}(-A_r + A_l + B_r - B_l) = \alpha(A_r + A_l) \tag{B.3}$$

We now identify A_l with the reflected amplitude r_δ , and B_r with the transmission amplitude t_δ. By setting the incoming amplitude $A_r = 1$, and assuming no reflection $B_l = 0$, we may combine these two equations(put numbers in) to obtain:

$$r = \frac{-1}{1 - \frac{2}{i\alpha k_n}} \tag{B.4}$$

$$t = \frac{1}{1 - \frac{i\alpha k_n}{2}} \tag{B.5}$$

This yields the reflection and transmission probabilities:

$$R = |r|^2 = \frac{1}{1 + \frac{4}{\alpha^2 k_n^2}} \tag{B.6}$$

$$T = |t| = \frac{1}{1 + \frac{\alpha^2 k_n^2}{4}} \tag{B.7}$$

Let us now rewrite the transmission amplitude in polar form:

$$t = \frac{1}{1 - \frac{i\alpha k_n}{2}} = \frac{1 + \frac{i\alpha k_n}{2}}{1 + \frac{\alpha^2 k_n^2}{4}} = \frac{e^{i \arctan(k\alpha/2)}}{\sqrt{1 + \frac{\alpha^2 k_n^2}{4}}} \tag{B.8}$$

Consider now a similar derivation for the finite mirror model. Again we send a plane wave towards the central mirror from the left. Let n be the index of refraction, and $2M$ be the width of the finite mirror. The plane wave will then have the form:

$$E_n(x) = \begin{cases} e^{ik_n x} + re^{-ik_n x} & x < -M \\ C_1 e^{ink_n x} + C_2 e^{-ink_n x} & -M < x < M \\ te^{ik_n x} & x > M \end{cases} \tag{B.9}$$

Imposing continuity across the two surfaces gives:

$$e^{-ik_n M} + re^{ik_n M} = C_1 e^{-ink_n M} + C_2 e^{+ink_n M} \tag{B.10}$$

$$C_1 e^{ink_n M} + C_2 e^{-ink_n M} = te^{ik_n M} \tag{B.11}$$

We also require continuity of the first derivative across the surfaces:

$$ike_n^{-ik_n M} - ik_n re^{ik_n M} = ink_n C_1 e^{-ink_n M} - ink_n C_2 e^{+ink_n M} \tag{B.12}$$

$$ink_nC_1e^{ink_nM} - ink_nC_2e^{-ink_nM} = ik_nte^{ik_nM} \tag{B.13}$$

From these four equations we solve for the finite barrier transmission amplitude t_{FB} and find:

$$t_{FB} = \frac{1}{\cos(2nk_nM) - i\left(\frac{n^2+1}{2n}\right)\sin(2nk_nM)} \tag{B.14}$$

Rewriting this in polar coordinates:

$$t_{FB} = \frac{1}{\cos(2nk_nM) - i\left(\frac{n^2+1}{2n}\right)\sin(2nk_nM)} \frac{\cos(2nk_nM) + i\left(\frac{n^2+1}{2n}\right)\sin(2nk_nM)}{\cos(2nk_nM) + i\left(\frac{n^2+1}{2n}\right)\sin(2nk_nM)} \tag{B.15}$$

$$= \frac{e^{i\arctan\left(\frac{n^2+1}{2n}\tan(2nk_nM)\right)}}{\sqrt{1+\left(\frac{n^2-1}{2n}\right)^2\sin^2(2nk_nM)}} \tag{B.16}$$

Comparing the amplitudes of t_{FB} with t_δ we find that:

$$\alpha k_n = \frac{n^2-1}{n}\sin(2nk_nM) \tag{B.17}$$

Comparing the phase of t_{FB} with that of t_δ:

$$\alpha k_n = \frac{n^2+1}{n}\tan(2nk_nM) \tag{B.18}$$

Therefore we see that by matching the reflection or transmission of the two models, we are not in fact matching the phase of the transmitted waves.

This leads to perturbations in the wavenumbers and accounts for the variability between the delta and finite barrier models.

Appendix C

The diabatic basis

The solution of the transcendental equation (2.6) allows us to construct global modes which exist throughout the double cavity. The global modes are the eigenvectors of the time-independent Maxwell wave equation in the double cavity. These modes give the so-called adiabatic basis as specified by Eqns (3.4) and (3.5), and we denote this basis by $U_e(x)$ and $U_o(x)$.

It is convenient to be able to express the double cavity problem in a basis which we refer to as the "LZ diabatic basis", or the "diabatic basis" for short. We *define* the diabatic basis as the basis in which solutions to the time-independent Maxwell/Schrödinger wave equation can be expressed in the form given by the LZ Hamiltonian matrix (3.1). In other words, the diabatic energies $\pm E(t)$ and eigenvectors are those found from the LZ Hamiltonian when $\Delta = 0$. We shall denote the diabatic basis vectors $\phi_L(x)$ and $\phi_R(x)$.

The situation now is that we already know the adiabatic basis and need to find the diabatic basis. We now preform an "undiagonalization" into the specific LZ form (3.1), which may easily be achieved by rotating the states correctly.

We begin from the diagonalized LZ matrix (i.e. LZ Hamiltonian in the adiabatic basis)

$$H_{\text{ad}} = \begin{bmatrix} E_+(t) & 0 \\ 0 & E_-(t) \end{bmatrix} \tag{C.1}$$

where $E_\pm = \pm\sqrt{E^2 + \Delta^2}$ are the adiabatic energies (global wavenumbers), where the plus sign corresponds to the solution which is even at $\Delta L = 0$. We want to transform this matrix into the LZ matrix in the diabatic basis

$$H_{LZ} = \begin{bmatrix} E(t) & \Delta \\ \Delta & -E(t) \end{bmatrix} . \tag{C.2}$$

In order to go between (C.1) and (C.2) we perform a similarity transformation. Let $H_{\text{ad}} =$

$S^{-1}H_{LZ}S$, where

$$S = \begin{bmatrix} \cos\theta & \sin\theta \\ -\sin\theta & \cos\theta \end{bmatrix} . \tag{C.3}$$

We find that the matrix elements of S are given by

$$\cos\theta = \sqrt{\frac{\sqrt{E^2+\Delta^2}+E}{2\sqrt{E^2+\Delta^2}}} = \sqrt{\frac{E_+ + \sqrt{E_+^2-\Delta^2}}{2E_+}} \tag{C.4}$$

and

$$\sin\theta = -\sqrt{\frac{\sqrt{E^2+\Delta^2}-E}{2\sqrt{E^2+\Delta^2}}} = -\sqrt{\frac{E_+ - \sqrt{E_+^2-\Delta^2}}{2E_+}} \tag{C.5}$$

where the expressions after the second equality in both equations are written in terms of the adiabatic quantities obtained by solving the transcendental equation (2.6). In particular, the value of Δ is found from $\Delta = E_+|_{\Delta L=0}$.

The relationship between the two sets of basis states is then

$$\phi_R(x) = \cos\theta\ U_e(x) + \sin\theta\ U_o(x) \tag{C.6}$$

$$\phi_L(x) = -\sin\theta\ U_e(x) + \cos\theta\ U_o(x) \tag{C.7}$$

and conversely

$$U_e(x) = \cos\theta\ \phi_R(x) - \sin\theta\ \phi_L(x) \tag{C.8}$$

$$U_o(x) = \sin\theta\ \phi_R(x) + \cos\theta\ \phi_L(x)\ . \tag{C.9}$$

The orthogonality relations satisfied by $\phi_{L/R}$ can be found by substituting Eqns (C.8) and (C.9) into Eq. (2.1). One finds

$$\frac{1}{\varepsilon_0}\int_{-L_1}^{L_2} \varepsilon(x)\phi_{L/R}(x)\phi_{L/R}(x)dx = 1 \tag{C.10}$$

$$\frac{1}{\varepsilon_0}\int_{-L_1}^{L_2} \varepsilon(x)\phi_L(x)\phi_R(x)dx = 0\ . \tag{C.11}$$

Appendix D

Analytic Approximation for Wavenumbers

We derive expressions for wavenumbers $k_{n,e}$ and $k_{n,o}$ given in equations (2.13) and (2.14). When $\Delta L = 0$ the odd wavenumber solution must match the local mode solution given by

$$k_{n,0}(\Delta L = 0) = \frac{2n\pi}{L} \tag{D.1}$$

Consider now the wavenumber transcendental equation (2.7)

$$\cos(k\triangle L) - \cos(kL) = 2\frac{\sin kL}{\alpha k} \tag{D.2}$$

For higher lying wavenumbers (i.e in the optical range), the sinc function $\frac{\sin kL}{\alpha k}$ will be small, and hence $k_{n,e}$ at $\Delta L = 0$ should be near $\frac{2n\pi}{L}$. We therefore expand the sinc term to second order about $\frac{2n\pi}{L}$ and do the same to the $1 - \cos(kL)$ term. This yields

$$\frac{1}{2}(Lk_{n,e} - 2n\pi)^2 = \frac{2L}{\alpha}\left(\frac{(Lk_{n,e} - 2n\pi)}{2n\pi} - \frac{(Lk_{n,e} - 2n\pi)^2}{(2n\pi)^2}\right) \tag{D.3}$$

Solving for $k_{n,e}$ we get

$$k_{n,e}(\Delta L = 0) = \frac{2\pi n}{L} + \frac{1}{2\pi n}\frac{1}{\frac{\alpha}{4} + \frac{L}{(2\pi n)^2}} \tag{D.4}$$

We now want an expression for $k_{n,e}$ and $k_{n,o}$ as a function of ΔL in the neighborhood of $\Delta L = 0$. We want a second order expression of the form

$$k_{n,e/o}(\Delta L) \approx k_n(0) + \left[\frac{\partial}{\partial(\Delta L)}k_n(0)\right]\Delta L \pm \frac{1}{2}\left[\frac{\partial^2}{\partial(\Delta L)^2}k_n(0)\right]\Delta L^2 \tag{D.5}$$

In order to find the derivatives of k_n, we differentiate the transcendental equation (2.7) with respect to ΔL twice and isolate terms. The first derivative will be zero as we are at a maximum/minimum point for $k_{n,e/o}$ when $\Delta L = 0$. The second derivative evaluated at $\Delta L = 0$ is found to be:

$$\frac{\partial^2}{\partial(\Delta L)^2} k_n(0) = \frac{\alpha(2n\pi)^3}{2L^4} - \frac{\alpha(2n\pi)}{2L^4} \approx \frac{\alpha(2n\pi)^3}{2L^4} \tag{D.6}$$

Note this was done for $k_{n,o}$ where we used the fact that $k_{n,0}(\Delta L = 0) = \frac{2n\pi}{L}$. For the even wavenumber, we expect the curvature to be very near this (with opposite sign) and we make that approximation here. Therefore, to second order we have

$$k_{n,e} = \frac{2\pi n}{L} + \frac{1}{2\pi n} \frac{1}{\frac{\alpha}{4} + \frac{L}{(2\pi n)^2}} + \frac{2\pi^3 n^3 \alpha \Delta L^2}{L^4} \tag{D.7}$$

$$k_{n,o} = \frac{2\pi n}{L} - \frac{2\pi^3 n^3 \alpha \Delta L^2}{L^4} \ . \tag{D.8}$$

Appendix E

The Maxwell wave equation in a moving dielectric

Leonhardt and Piwnicki [25] have given a modification of Maxwell's wave equation, based upon ideas originally due to Fresnel, appropriate for light propagating in a slow moving, dispersionless, dielectric medium

$$\left(\nabla^2 - \frac{n_r^2}{c^2}\frac{\partial^2}{\partial t^2} - 2\frac{n_r^2-1}{c^2}\mathbf{v}.\nabla\frac{\partial}{\partial t}\right)\mathcal{E}(\mathbf{x},t) = 0\,, \tag{E.1}$$

where $n_r(x,t) = \sqrt{\varepsilon(x,t)/\varepsilon_0}$ is the refractive index. This equation is written in frame in which the dielectric is observed to move with a velocity $\mathbf{v}$, and is correct to first order in $|\mathbf{v}|/c$. In our case the moving dielectric medium is the common mirror. Our aim here is to estimate the size of the final term in the brackets: the maximum size it can take is if the derivatives act on the phase of the electric waves, i.e. $\nabla \to k$ and $\partial/\partial t \to \omega_{\rm av}$. Then the magnitude of this term is $k^2(n_r^2-1)(v/c)$. For the validity of our treatment in Section 3.2 to hold, this should be much smaller than the smallest term we keep in our reduction of the Maxwell wave equation to a first order in time Schrödinger-like equation. Referring to Eq. (3.28), we see that the smallest term we keep is $\beta_{L/R}\dot{\tilde{A}}_{L/R}$, where $\beta_{L/R} \approx \omega_{\rm av}$. In Section 3.2 we argue that this term has a magnitude of $\beta_{L/R}\dot{\tilde{A}}_{L/R} \approx \omega_{\rm av}(\Delta/\hbar) = 10^{27}{\rm s}^{-2}$, and thus $\beta_{L/R}\dot{\tilde{A}}_{L/R}/c^2 \approx 10^{10}{\rm m}^{-2}$. This is considerably larger than $k^2(n_r^2-1)(v/c) \approx 10^6{\rm m}^{-2}$.

Bibliography

[1] *Quantum information science and technology road mapping project*, Los Alamos National Laboratory, 2006. [Online]. Available: http://qist.lanl.gov/qcomp map.shtml

[2] H. J. Kimble, Nature **453**, 1023 (2008).

[3] D. P. Divincenzo, Fortschritte der Physik, **48**, 771 (2000).

[4] J. I. Cirac, P. Zoller, H. J. Kimble, and H. Mabuchi, Phys. Rev. Lett., **78**, 3221 (1997).

[5] K. Bergmann, H. Theuer, and B. W. Shore, Rev. Mod. Phys. **70**, 1003 (1998).

[6] G. Heinrich, J. E. Harris and F. Marquardt, Phys. Rev. A **81** 0118010 (2010).

[7] I. E. Linington, Ph.D. thesis, University of Sussex (unpublished, 2006).

[8] I. E. Linington and B. M. Garraway, J. Phys. B: At. Mol. Opt. Phys. **39**, 3383 (2006).

[9] I. E. Linington and B. M. Garraway, Phys. Rev. A **77**, 033831 (2008).

[10] L. Landau, Phys. Z Soviet Union, **2**, 46 (1932).

[11] C. Zener, Proc. Roy. Soc. of London Series A **137**, 696 (1932).

[12] S. Stenholm in *Quantum Dynamics of Simple Systems*, edited by G.-L. Oppo, S. M. Barnett, E. Riis and M. Wilkinson (IOP, Bristol, 1996).

[13] R. Lang, M. O. Scully and W. E. Lamb, Phys. Rev. A **7**, 1788 (1973).

[14] L. D. Landau and E. M. Lifshitz, *Quantum Mechanics* Third edition (Butterworth-Heinemann, Oxford, 1977).

[15] http://www.physikinstrumente.com

[16] F. Brennecke, T. Donner, S. Ritter, T. Bourdel, M. Köhl, and T. Esslinger, Nature (London) **450**, 268 (2007).

[17] Y. Colombe, T. Steinmetz, G. Dubois, F. Linke, D. Hunger, and J. Reichel, Nature (London) **450**, 272 (2007).

[18] M. Trupke, J. Goldwin, B. Darquié, G. Dutier, S. Eriksson, J. Ashmore, and E. A. Hinds, Phys. Rev. Lett. **99**, 063601 (2007).

[19] K. W. Murch, K. L. Moore, S. Gupta, and D. M. Stamper-Kurn, Nature Phys. **4**, 561 (2008).

[20] M. V. Berry and K. E. Mount, Rep. Prog. Phys. **35**, 315 (1972).

[21] J. M. Raimond, M. Brune, and S. Haroche, Rev. Mod. Phys. **73**, 565 (2001); H. Walther, B. T. H. Varcoe, B.-G. Englert, and T. Becker, Rep. Prog. Phys. **69**, 1325 (2006).

[22] A. Wallraff *et al.*, Nature **431**, 162 (2004); I. Chiorescu *et al.*, Nature **431**, 159 (2004); J. Johansson *et al.*, Phys. Rev. Lett. **96**, 127006 (2006); A. Blais, R. S. Huang, A. Wallraff, S. M. Girvin, and R. J. Schoelkopf, Phys. Rev. A **69**, 062320 (2004).

[23] L. I. Schiff, *Quantum Mechanics* Third Edition (McGraw-Hill, New York, 1968).

[24] M. Abramowitz and I. Stegun, *Handbook of Mathematical Functions*, (National Bureau of Standards, Washington, 1964).

[25] U. Leonhardt and P. Piwnicki, Phys. Rev. A **60**, 4301 (1999).